Progress in
Physical Geography

Was the Little Ice Age the coolest Holocene climatic period in the Italian central Alps?

Journal:	*Progress in Physical Geography*
Manuscript ID	PPG-19-045.R2
Manuscript Type:	Main Article
Keywords:	Polycyclic palaeosols, Frost pedofeatures, Mid-Late Holocene, Little Ice Age, Southern Alps, Micropedology

Abstract:	Estimation of the relative intensity of different cold periods occurring during the Late Quaternary are difficult tasks, particularly in non-glaciated mountain landscapes, and where high- to medium-resolution archives for proxy data are lacking. In this paper, we study a Holocene polycyclic soil sequence in the central Alps (Val Cavargna, Northern Italy) to estimate climatic parameters (specifically T) changes in non-glaciated, high altitude environments. We investigate this key site through palaeopedological and micromorphological analyses in order to understand phases of soil development and detect hidden evidence of cold conditions during its formation. Three phases of pedogenesis can be recognized and attributed in time to different periods during the Holocene. Pedogenetic phases were separated by two truncation and deposition episodes related to the reactivation of slope processes under cold conditions at the onset of the Neoglacial and the Iron Age Cold Epoch (IACE) respectively. Micromorphological evidence of frost action on soil can instead relate to pedogenetic processes acting in the Little Ice Age (LIA). The different expression of these three cold periods corresponds to different climatic conditions, pointing to the LIA as a cooler/drier period in comparison to the preceding ones.

Was the Little Ice Age the coolest Holocene climatic period in the Italian central Alps?

Abstract

Estimation of the relative intensity of different cold periods occurring during the Late Quaternary are difficult tasks, particularly in non-glaciated mountain landscapes, and where high- to medium-resolution archives for proxy data are lacking. In this paper, we study a Holocene polycyclic soil sequence in the central Alps (Val Cavargna, Northern Italy) to estimate climatic parameters (specifically T) changes in non-glaciated, high altitude environments. We investigate this key site through palaeopedological and micromorphological analyses in order to understand phases of soil development and detect hidden evidence of cold conditions during its formation. Three phases of pedogenesis can be recognized and attributed in time to different periods during the Holocene. Pedogenetic phases were separated by two truncation and deposition episodes related to the reactivation of slope processes under cold conditions at the onset of the Neoglacial and the Iron Age Cold Epoch (IACE) respectively. Micromorphological evidence of frost action on soil can instead relate to pedogenetic processes acting in the Little Ice Age (LIA). The different expression of these three cold periods corresponds to different climatic conditions, pointing to the LIA as a cooler/drier period in comparison to the preceding ones.

Keywords

Polycyclic palaeosols; Micropedology; Frost pedofeatures; Mid-Late Holocene; Little Ice Age; Southern Alps.

I. Introduction

One of the most difficult tasks in paleoclimate studies – before the introduction of instrumental measurements – is the estimation of climate parameters and their variation with time (Edwards et al., 2007a; Bradley, 2015). When records are irregular and limited to shortened time-spans, discontinuous or low in resolution, such as in many continental palaeoenvironmental archives, the reconstruction of climatic conditions and their effects on the landscape becomes much more challenging (Kutzbach, 1976; Federici, 2005; Giraudi et al., 2011; Bradley, 2015; Furlanetto et al., 2018). This is especially true when dealing with the effects of cold periods in middle latitude and Mediterranean mountain ranges, such as the Alps and Apennines of Italy, known as highly dynamic regions (Porter and Orombelli 1985; Baroni and Orombelli 1996; Federici, 2005; Hughes et al., 2011; Kuhlemann et al., 2013; Pelfini et al., 2014; Colucci et al., 2016; Bollati et al., 2018). Where extensive landforms and stratigraphic records of Quaternary glacial advances are not present, evident traces of cold phases are often hard to study. Poorly visible, buried and hidden signs of cold periods – as much as of the subsequent warm phases – are only occasionally embedded and rarely well-preserved in landforms and within palaeosols and sedimentary records (Angelucci et al., 1992; Calderoni et al., 1998; Fischer et al., 2012; Compostella et al., 2012, 2014; Waroszewski et al., 2018). In the latter, evidence of cold phases is often associated with breaks in the sedimentary succession or with an increased frequency of slope processes related to climatic instability (Bertolini et al., 2004; Nicolussi et al., 2005; Magny et al., 2009a; Arnaud et al., 2012; Cremaschi and Nicosia, 2012; Compostella et al., 2014; Pelfini et al, 2014; Mariani et al., 2019). Despite the extensive documentation regarding the Little Ice Age (LIA) traced in paleoclimate studies (Kullman and Öberg, 2009; Arnaud et al., 2012; Nicolussi, 2013; Carturan et al., 2014; Loso et al., 2014), many questions are still open, for example , the influence of climate variations on non-glaciated mountain landscapes during the LIA is poorly known, especially when compared to previous cold intervals such as the Neoglacial, the Lateglacial, and the Last Glacial Maximum (LGM) (e.g., Wanner et al., 2011; Badino et al., 2018; Furlanetto et al., 2018). In the mountain environments of middle latitudes, where glacial and periglacial landforms are undetectable or have been vanished/truncated/erased due to enhanced slope activity (e.g.: Allison, 1996; Giraudi et al., 2011; Compostella et al., 2014; Mariani et al., 2018), paraglacial (Knight and Harrison, 2009), or zoogeomorphological processes (e.g., Butler, 1995, 2012), the effects of cold phases are virtually absent from the scientific record.

In this paper, we studied a Holocene polycyclic soil sequence formed in the Mid-Late Holocene in the Italian Central Alps (Val Cavargna, CO). Our aim is to find records of Holocene climatic influence on the evolution of surface processes (Nicholson, 1988), and to assess whether soils and paleosols (and their pedofeatures) can record climatic changes in Alpine environments. The studied soil sequence shows clear traces of the presence of cold conditions during its formation, strong enough to promote soil frost and trigger the formation of frost-induced pedofeatures (*sensu* Van Vliet-Lanoë, 1998; Van Vliet-Lanoë et al., 2018) without the influence of glacial or periglacial processes. No evidence for glacials were found at the study site and in its close vicinity. Using multiple palaeopedological techniques, and in particular micropedology, we were able to characterize different Holocene cold phases affecting soil formation. We also stress the impact as a climatic parameter of different atmospheric temperatures during the cold periods of the last few millennia. We lastly suggest an alternative qualitative approach to interpret past fluctuations of climatic parameters based on their effect on surface processes.

II. The study area

The studied soil sequence is located at Alpe Piazza Vacchera (46°06′32′′N, 9°08′33′′E), in Val Cavargna (San Bartolomeo municipality, Italian Central Alps), at an elevation of 1680 m a.s.l. (Figures 1 and 2). The bedrock of the studied area is part of a portion of the Southalpine basement – the tectono-metamorphic unit of the Dervio–Olgiasca Zone (after Spalla et al., 2002) – and consists mainly of garnet-staurolite-bearing schist and minor gneiss with lenses of amphibolite. Schists are particularly prone to weathering, especially in areas of pervasive jointing due to tectonic deformation. The study site is currently above the treeline and covered by grassland pastures; mean annual rainfall is between 2000–2500 mm/y and mean annual temperature between 3.8 and 10.9°C (Ceriani and Carelli, 2000). Snow accumulation is high, estimated between 1–2 m/y, with a residence time greater than 100 days (Gazzolo and Pinna, 1973). The permanent snow line for the Alps varies from N to S and from W to E according to factors related to latitude, continentality and slope insulation, but it is generally located between 2500–2800 m a.s.l. (Barry, 1992), thus well above the area of study. The area does not contain permafrost: in this portion of the Alps favourable conditions for permafrost are found only above 2200–2300 m a.s.l. (Boeckli et al., 2012), and the first instances of permafrost or related landforms are found in a range of tens of kilometres to the North (Cremonese et al., 2011). During the LGM, valley glaciers did not cover the area but at least a few cirque or slope glaciers were present in the highest part of the mountain range (Bini et al., 2009). Since then, no traces of further glacial influence are found on the slopes or in the valley below (Bini et al., 2009). Periglacial processes are visible as sparse, possibly inactive solifluction lobes on the surrounding slopes, today highly disturbed by zoogeomorphologically induced game trails, causing instability and enhanced gully erosion and transportation of soil material in the vicinity of the studied area (e.g., Butler, 2018; Zerboni and Nicoll, 2018).

Human activity in Val Cavargna is known since the Mesolithic, with the establishment and abandonment of sporadic settlements in the upper part of the valley. Subsequent occasional occupation of the area with evidence of widespread forest fires took place multiple times from the Neolithic to the Middle Ages (Castelletti et al., 2012a). The systematic exploitation of the area, resulting in an increase in human pressure on the landscape, dates back mainly to post-medieval times (Castelletti and Tremari, 2012). Documented instances of forest clearance in the upper valley appear since the XVI century CE, with a change in land use for charcoal production (Grandi, 2012). At this time, large portions of deforested land – between 1400-1800 m a.s.l. – were converted to pasture lands (Castelletti et al., 2012b). Near the studied section, the first establishment of a small cattle farm and trail can be loosely attributed to the same period.

III. Materials and methods

To investigate the soil in the field we dug a trench along the western slope of Mount Pianchette – Pizzo di Gino, in correspondence of a natural filled trench forming a small terrace on a deep-seated gravitational slope deformation (DSGSD). This landform represents large to extremely large mass movements generally affecting the entire length of high-relief valley flanks, extending up to 200–300 m in depth, which can frequently extend beyond the slope ridge (Crosta et al., 2013). Soil descriptions and horizon designations were carried out according to the guidelines of FAO (2006); colour definition followed the Munsell Color® (1994) nomenclature. The diagnostic horizons of buried palaeosols in the sequence were defined according to the international classification systems (FAO, 2014; Soil Survey Staff, 2014; Zerboni et al., 2011, 2015). Soil samples for chemical-physical analyses were collected for each horizon. Particle size distribution was determined using laser diffraction (Malvern Mastersizer MS-2000) after H_2O_2 and HCl treatments, according to the procedure described in Crouvi et al. (2008). The total amount of Fe and Al in the samples was determined by complete dissolution in a mixture of HF, HCl, HNO_3 and $HClO_4$, followed by measurement of the solubilised ions using an ICP-ES (Jobin-Yvon JV24). Dithionite- (Mehra and Jackson, 1960) and oxalate-extractable (McKeague et al., 1971; Schwertmann, 1973) fractions of Fe and Al oxyhydroxides, representing a quantification for free and amorphous Fe and Al forms respectively, were also measured with the same instrument. The Activity Ratio between oxalate- and dithionite-extractable iron (Fe(o)/Fe(d)) was also calculated. Analytical data are reported in Table 1 and summarized in Figure 3.

Thin sections were produced from undisturbed samples taken from relevant soil horizons after impregnation with polyester resin according to the method described in Murphy (1986). Slides were examined with an Olympus BX41 petrographic microscope, under plane-polarized light (PPL), cross-polarized light (XPL), and oblique incident light (OIL). The terminology of Stoops (2003) was used to describe thin sections, whereas micromorphological interpretation was mainly based on the concepts reported in Stoops et al. (2018).

The age of the polycyclic soil sequence was obtained by dating with radiocarbon (AMS-^{14}C) two samples of charcoal. AMS-^{14}C dating results were calibrated (2σ range) using the INTCAL13 curve (Reimer et al., 2013).

IV. Results

Along the slope of Mt. Pianchette and Mt. Pizzo di Gino, inside the morphological trench formed by a detachment niche of a DSGSD, are present a series of shallow depressions filled with sediments deposited through colluvial slope processes that were subsequently weathered and reorganized into soils. In the uppermost depression, several soil horizons were identified (Table 1), consisting of three different soil units on successively deposed parent materials (Figure 2). The uppermost unit corresponds to the extant soil, down to a depth of about 49 cm. It is an organic temperate mountain soil differentiated in thicker organic A horizons sometimes alternated with thinner levels of rubified soil material containing dark mottles. The same material is also present at the bottom of the unit as a mineral Bw horizon. The boundary between this unit and the intermediate one is marked by an erosional surface bearing a residual lens of macroscopic charcoal fragments, several centimetres thick, identified as the remains of a fireplace. Dating from two charcoal samples taken from this lens gave a result of 2730±43 (RC-369) and 2683±42 (RC-370) years uncal BP (2926–2756 years cal BP and 2863–2747 years cal BP respectively). The intermediate unit is a buried palaeosol divided into three main horizons: an eluvial 2E horizon occupies the upper position above a rubified 2Bs horizon; below them is a mineral 2BC horizon with common reddish mottles. The lowermost soil unit, starting at a depth of 75 cm, is quite similar to the previous one, but pedofeatures are better expressed. A whitish eluvial 3Et horizon, in which are still present reddish mottles comparable to those of the level above it, forms the upper portion of the unit, followed by a weathered rubified 3Bs horizon. Below the latter, a 3C horizon marks the boundary to the bedrock at about 130 cm below the current surface. Charcoal fragments from the 3Bs horizon of this unit were dated to 6850±20 years uncal BP (UGAMS-38048, 7721–7621 years cal BP).

Grain size analytical data from a selection of soil samples shows where units differ and where instead similarities emerge (Figure 3). The A2 horizon of the top unit differs from the others, showing a bimodal distribution of grain size classes: the main mode is represented by silt, while a secondary mode is shifted towards medium/coarse sand. Its much broader distribution also indicates a poor selection of grains. Horizons from the other two units show very similar categories. In particular, the E horizons share almost the same bell curve weakly skewed to the left and centred on coarse silt. All B horizons (Bw, 2Bs and 3Bs) also share a similar trend with a mode at the fine sand and a higher skewness towards the finer fractions that are more expressed in the bottom unit. Total iron content in the soil sequence amounts to 3-5.5% of the total mass in all soil horizons, with concentrations in the B horizons of the top and bottom units (Figure 3; Table 1). Eluvial horizons show lower concentrations of Fe, with the 3Et horizon being the scarcest in total iron content (3.06%). The intermediate unit is also low in iron content, with only a slight increase of total iron in the 2B horizon. Free iron measured as Fe-dithionite peaks in the Bw and 3B horizons and shows the lowest concentration at the bottom of the sequence (11.6 g/kg in the 3C horizon); generally, free iron accounts for 47-71% of total iron content. The Activity Ratio is mostly between 0.35 and 0.5 for all horizons, with the exception of E horizons where it reaches the lowest values (below 0.3).

The observation of thin sections reveals the general composition and fabric of the soil units (Table 2). The micromass of all investigated horizons shows a dominance of coarse mineral material (mainly micas, then quartz and feldspar) with the fine material either compactly filling the remaining space in B horizons (Figure 4a), or weakly aggregating in granular peds in E horizons (Figure 4b). Fine charcoal is always present; coarser fragments can be found in the A1 and 3Et horizons as well as in the charcoal-bearing lens at the top of the 2E horizon. The 3Et horizon shows microlaminated clay coatings (Figure 4c, d) inside a groundmass with marked differences from the B horizons: the fine material bears a greyish colour and no visible aggregation is present. The A1 and A2 horizons are locally arranged in a pattern of horizontal planar voids (isoband fabric, *sensu* Dumanski and St-Arnaud, 1966), not visible in the deeper parts of the soil sequence (Figure 5a). This pattern is randomly distributed in the two horizons as large centimetric patches sharing the same features: a net of partially interconnected straight or slightly curved planar voids up to a millimetre long and less than 100 μm thick that separate lenses of soil material up to 1 mm thick. Vesicles are often associated with soil lenses (Figure 5b) and the pattern itself. Clusters of parallel-oriented coarse fragments (Figure 5c) are visible in the Bw horizon. All these features are usually undisturbed by the presence of bioturbation otherwise found in many instances in the soil mass in the form of passage features (Figure 5d).

V. Discussion

In the following parts we reconstruct the evolution of the investigated soil sequence discussing the main pedogenetic processes involved in its formation. We then highlight the occurrence of pedofeatures in the different soil units that record past temperature shifts in the area.

5.1. Soil forming processes and chronology

The characterization of pedogenesis in the three units shows evidence of similar soil formation processes in different periods of time, thus confirming the existence of a soil polysequence (Cremaschi and Rodolfi, 1991). The very similar grain sizes of the different horizons imply that each soil unit was formed by deposition over the previous surface – exposed by truncation – of the same type of sediments removed from above by short-range (tens to hundreds of metres) slope transportation movements. Each soil unit shares the combined presence of an E/B horizon series, with the E substituted by a moderately depleted A2 horizon in the uppermost unit. The formation of clay and Fe oxyhydroxides in the soil mass is accompanied by their translocation downwards from the eluvial horizons into the lower rubified B horizons, or even below in older soil units, as in the case of the clay coatings that crossed the boundary into the 3Et horizon. Particle translocation is also supported by the shift from the 2Bs to the 3Et horizon, which hints to clay depletion from the second unit and illuviation into the unit below, and by the enrichment in fine material in the 3Bs horizon. The low activity ratio shows a relative depletion in the amorphous iron forms, easier to mobilise, in E horizons. The three units show different degrees of the same pedogenetic processes pedoplasmation, soil formation by weathering and translocation of clay minerals and Fe oxyhydroxides; Duchaufour, 1983), decreasing in strength of expression upwards. In fact, although the bottom unit looks the most developed in a well-defined series of horizons, Fe oxyhydroxides do not change markedly along the units, showing again uniformity in weathering. Pedogenesis is in any case only moderately developed, and the accumulation of Fe in the B horizons appears to be not only a result of in-situ weathering, but also of translocation from the overlying horizons and younger parent materials (Duchaufour, 1977; Cornell and Schwertmann, 2003).

Pedogenesis occurred under warm/temperate climate phases with the presence of continuous vegetation (Duchaufour, 1983) and promoted the accumulation of microlaminated clay coatings by illuviation into the unit below (e.g. Fedoroff, 1997; Compostella et al., 2014). The microstructure of E horizons and the presence of red mottles in B horizons (Table 3) suggest an incipient podsolization process (Duchaufour, 1983; Van Ranst et al., 2018), likely supported by local conditions of seasonal water saturation (Duchaufour, 1983; Sevink and de Waal, 2010; Vepraskas et al., 2018). The identification of wood species from charcoal fragments found in various soil horizons shows the dominance of silver fir (*Abies alba*) throughout the soil sequence: reconstructions of the vegetation history of the area point to the presence of an open forest under moderately warm conditions (Castelletti et al., 2012b). At the current surface and towards the top of the intermediate unit, charcoal assemblages suggest a sparsely forested heathland, revealing colder phases of forest retreat or anthropogenic pressure (Castelletti et al., 2012b).

Radiocarbon dating stresses formation of the various soil units within the Holocene, showing how the soil sequence has in fact experienced more than one warm climate phase. The development of the bottom unit, dated to 7721–7621 years cal BP, can be very clearly attributed to the Early-Middle Holocene (Mayewski et al., 2004; Arnaud et al., 2012; Grosjean et al., 2007), during a warm period preceding the cold event at 4.2 ka cal BP (e.g., Zanchetta et al., 2016), possibly the Atlantic Warm Period (AWP) or the Late Neolithic Thermal Maximum (LNTM). In this longer period of pedogenesis, potentially lasting a few thousands of years, the soil had the time to develop pedofeatures under a rapidly warming phase. Afterwards, the warm and stable phase responsible for the formation of the intermediate unit should occur after the Middle/Late Holocene transition, when several warm fluctuations occurred (Mayewski et al., 2004; Deline and Orombelli, 2005): the longest phase takes place during the Bronze Age, loosely between 3800 and 2800 years BP (e.g., Arnaud et al., 2012 and references therein), and can be confirmed by dating from the truncation of the unit indicated by the residual fireplace (2926–2756 and 2863–2747 years cal BP). It is therefore possible that this pedogenesis took place in a period not much longer than a thousand years. The truncation points to the transition from a warm period to the next cold phase (Plunkett and Swindles, 2008; Magny et al., 2009b; Wanner et a., 2011; Regattieri et al., 2014; Cremaschi et al., 2016) corresponding to the Iron Age Cold Epoch (IACE). This cold stage probably witnesses both the truncation of the intermediate unit due to enhanced slope processes and the deposition of the parent material composing the top one. The last phase of pedogenesis probably started since the Roman Warm Period (RWP) onwards to present time, covering less than 2000 years of duration in a fluctuating climate.

5.2. Are frost-related pedofeatures a proxy for past temperatures?

The typical pedofeatures found at the top unit (A1-A2 horizons) relate to specific climate conditions and can be safely attributed to a post-RWP cold phase on the basis of the above-mentioned chronological framework. The LIA is most likely the coldest climatic phase in that time interval (Wanner et al., 2011; Furlanetto et al., 2018). The pattern of microscopic horizontal planar voids separating the matrix into homogeneous lenses of soil material indicates the action of frost on soil horizons (Dumanski and St-Arnaud, 1966). Vesicles are also related to the entrapment of air bubbles in the soil mass during the freezing process (Table 3). As suggested by Van Vliet-Lanoë (1987, 1998) and Van Vliet-Lanoë et al. (2018), this regular pattern is connected to the presence of intermittent or seasonal frost episodes localised at the soil surface when the penetration of the freezing front is not very deep. This is expected for temperate environments, considering that very low air temperatures are needed to freeze the open ground below the first centimetres (Henry, 2007). Deformation of the soil mass is only limited to sporadic preferential orientations of coarse fragments, also indicating weak freezing conditions (Van Vliet-Lanoë et al., 1984). Nevertheless, the durability of these features to later pedo/bio-turbation (Van Vliet-Lanoë et al., 1984) indicates a certain level of stability compatible with repeated freeze-thaw cycles during an extended period.

The weak expression of the above described frost-related pedofeatures suggests the occurrence in the past of periglacial processes unrelated to permafrost (Van Vliet-Lanoë, 1998), the presence of which would have forced much stronger cryoturbation and very different features in the soil and is linked to more rigid conditions, possibly unmet here since the LGM. In fact, considering the stability through time of frost-related pedofeatures (Van Vliet-Lanoë et al., 1984), their absence in the two buried soil units suggests that frost acted in the area only during the most recent cold phase corresponding to the LIA, after the accumulation of the parent material of the uppermost soil unit. Since most of the pedogenetic factors identified by Jenny (1941) and the related soil-forming processes do not show dramatic changes over time, as seen above, this occurrence is probably more related to fluctuations in the climate. A climatic trend toward cooler conditions seems also confirmed by the general decrease in expression of pedogenetic processes from the bottom to the top of the pedosequence. This trend has been recently suggested from multi-proxy models of insolation at middle latitudes on alpine scale (Mauri et al., 2015). The supposed duration for each phase of soil formation, probably lasting several millennia to centuries, also needs to be taken into consideration. It is clear how time alone is not able to explain the differences in pedogenesis. In fact, both factors contributed in synergy to the development of soil formation processes (Boardman, 1985; Birkeland, 1999). We believe that in this case, while no simple comparison can be done between climate and time, the former seems to play the main role. The rapid succession of environmental changes in the Holocene represents the limiting factor in the development of pedogenesis. Time in this case cannot be the primary factor driving the expression of pedogenesis, since the different units are formed too suddenly because of the continuous climate shifts.

Considering the strong similarities in soil formation conditions between the three units, the effect of different cold periods on each is very noticeable. The abrupt truncation of the bottom unit could possibly correspond to the initial part of the Neoglacial period, often associated with a sharp increase in denudation processes (Arnaud et al., 2012). Denudation is in turn related to vegetation loss events often indirectly caused by the passage to cold and unstable climate phases (Bertolini et al., 2004; Nicolussi et al., 2005; Magny et al., 2009a; Compostella et al., 2014). Slope instability events responsible for the deposition of the two upper units are also a typical result of denudation processes, where erosion and deposition often occur consecutively on the same topographic surface (Giraudi et al., 2011; Compostella et al., 2014). The same appears to happen for the truncation of the second unit dated to the IACE (Magny et al., 2009b). For sake of clarity we need to consider that the anthropogenic contribution to the deposition and development of these units is not to be underestimated. Multiple fire events very likely connected to forest clearance practices started in the area since the Mesolithic (Castelletti et al., 2012b). Fire events greatly enhanced the effect of washout and solifluction on the slopes, mobilising the colluvial material that forms the two upper soil units. Human contribution to slope instability is in this case quite important, enhancing ongoing processes in synergy with the effect of climate variations. Later, also the zoogeomorphological effect due to the introduction of herding may have contributed to accelerate ongoing denudation and rill erosion.

The different setting of the uppermost unit, where frost features represent the effect of cold conditions in place of truncations, can be ultimately regarded as a distinct process attributed specifically to the LIA. Neoglacial cold events appear to have mainly impacted the soil through slope instability and processes of removal/addition of material, but no features directly related to freezing and ice formation are found at the top of the buried units. In this regard, while it is true that no actual surface A horizon is currently present on both units, it must be noted that the new surfaces produced by truncation were probably exposed to the weather for a non-insignificant length of time. On the intermediate unit this was enough to allow the establishment of a fireplace on top of the former topographic surface - or at least not far from it – which does not exhibit any visible frost feature. On the contrary, anthropogenic features as fireplaces are able to record frost-related pedofeatures (Cremaschi et al., 2015). The LIA has instead triggered in the soil a variety of stable features related to intermittent freezing cycles. Such clear difference might suggest that other climate dynamics were in place during the cold phases preceding the LIA (for instance, the

IACE). In this perspective, it might be plausible to characterise the LIA as a colder or drier period than the previous ones: lower temperatures in comparison with the other Holocene cold periods would have allowed more widespread episodes of seasonal frost. Holocene temperature anomalies reconstructed in the Southern Alps by Furlanetto et al. (2018) support this hypothesis suggesting a moderate shift towards lower temperatures in the LIA compared to other Holocene climatic phases. Moreover, a recent assessment of post-LGM permafrost distribution in the Mediterranean region suggests a widespread occurrence of soil frost in the LIA (Oliva et al., 2018). Similarly, a lessened amount of precipitation would have reduced the snow cover, well below the current thickness and down to only a few tens of centimetres (Zhang, 2005), weakening the thermal isolation of the soil below and allowing frost to take hold (Edwards et al., 2007b and references therein). A consequent shift downwards of the freezing front would plausibly have left more visible and stable features in the soils, while in less rigid and wetter phases they would only have suffered the consequences of more snow thawing upslope, especially a higher water discharge rate and in turn the activation of slope movements. The relationship between precipitation and slope processes is well studied in the Alps: today, where climate conditions are more severe lower rainfall thresholds are needed to trigger slope movements (Guzzetti et al., 2007). Considering the enhanced possibility of slope instability in cold environments, the absence of truncations in the upper soil unit confirms stable slope conditions and further supports a possible dry phase. While it is very difficult to assess past precipitation amount, reconstructed temperatures from proxy data in the Alps seem to favour this idea (for comparison, see Badino et al., 2018; Furlanetto et al., 2018). Similar conditions have also been very recently postulated for the Northern Apennines (Regattieri et al., 2014; Mariani et al., 2019). The occurrence of other evidence confirming the climatic conditions in Mediterranean mountain ranges during the LIA confirms that soils and pedofeatures can reflect regional climatic conditions and they are not only triggered by local conditions and surface processes. The effect of forest clearance must be taken into account when discussing temperature in the topsoil. In fact, the presence of a forest cover greatly mitigates the effect of air temperature on the soil, with the canopy protecting the lower air strata and producing a warmer microclimate that reaches temperatures below zero with more difficulty (Körner. 2003). On the other hand, the canopy effect also prevents part of the snow accumulation, reducing its isolating power. In this area, the continuous presence since the Mesolithic of clearance events by fire and the more recent establishment of pasturelands (Castelletti et al., 2012b) probably prevented for long periods of time the reestablishment of a closed forest, leaving more open vegetation in which both these effects were probably greatly reduced.

VI. Conclusions

This study reconstructs climatic fluctuations throughout the Holocene on the basis of a soil polysequence the pedogenetic processes that occurred in a high mountain range. Our study shows new evidence regarding the importance of the LIA in the Alps as one of the main cold intervals after the LGM. While it is difficult to make assumptions based on indirect archives, it is plausible to infer, based on the evidence found in this study, that during the LIA the intensity of frost action might have been stronger compared to other Holocene cold episodes. An increase in ice formation could in turn be related to the occurrence of drier/colder conditions weakening snow deposition on the soil surface and favouring overall freezing conditions.

While soil archives are considered a low-mid resolution resource in palaeoclimatic studies (Yaalon, 1990), in this case the reconstruction of pedogenesis was the only reliable tool for recording cold intervals that occurred after the LGM in a non-glaciated area and their influence on surface processes. The study of soils and specifically micromorphology discloses important information on past climate, where evidence of processes triggered by specific climatic and environmental conditions (in this case atmospheric temperature) can be observed and put inside their proper placement in time (*sensu* Cremaschi et al., 2018). In environments where human actions started tuning surface processes earlier than expected in the Mid-Late Holocene, as suggested by recent studies (ArchaeoGLOBE Project, 2019), soil evidence also helps in disentangling natural and anthropogenic factors shaping the landscape in human-settled contexts. The absence of deposits and landforms allowing the formation and conservation of soils and palaeosols would indeed render many of such reconstructions quite arduous, if not implausible.

References

Allison RJ (1996) Slope and slope processes. *Progress in Physical Geography* 20(4): 453-465.

Angelucci D, Cremaschi M, Negrino F and Pelfini M (1992) Il sito mesolitico di Dosso Gavia - Val di Gavia (Sondrio - Italia): evoluzione ambientale e popolamento umano durante l'Olocene antico nelle Alpi Centrali. *Preistoria Alpina* 28: 19–32.

ArchaeoGLOBE Project (2019) Archaeological assessment reveals Earth's early transformation through land use. *Science* 365: 897–902.

Arnaud F, Révillon S, Debret M, Revel M, Chapron E, Jacob J, Giguet-Covex C, Poulenard J and Magny M (2012) Lake Bourget regional erosion patterns reconstruction reveals Holocene NW European Alps soil evolution and palaeohydrology. *Quaternary Science Reviews* 51: 81-92.

Badino F, Ravazzi C, Vallè F, Pini R, Aceti A, Brunetti M, Champvillair E, Maggi V, Maspero F, Perego R and Orombelli G (2018) 8800 years of high-altitude vegetation and climate history at the Rutor Glacier forefield, Italian Alps. Evidence of middle Holocene timberline rise and glacier contraction. *Quaternary Science Reviews* 185: 41–68.

Baroni C and Orombelli G (1996) The Alpine "Iceman" and Holocene Climatic Change. *Quaternary Research* 46(1): 78 – 83.

Barry RG (1992) *Mountain weather and climate*. London: Routledge.

Bertolini G, Casagli N, Ermini L and Malaguti C (2004) Radiocarbon data on Lateglacial and Holocene landslides in the Northern Apennines. *Natural Hazards* 3: 645–662.

Bini A, Buoncristiani JF, Coutterand S, Ellwanger D, Felber M, Florineth D, Graf HR, Keller O, Schlüchter C and Schoeneich P (2009) *La Svizzera durante l' ultimo massimo glaciale (LGM), 1:500' 000*. Ufficio federale di topografia swisstopo, Wabern.

Birkeland PW (1999) *Soils and Geomorphology*. New York: Oxford University Press.

Boardman J (1985) Comparison of Soils in Midwestern United States and Western Europe with the Interglacial Record. *Quaternary Research* 23(1): 62-75.

Boeckli L, Brenning A, Grube S and Noetzli J (2012) Permafrost distribution in the European Alps: calculation and evaluation of an index map and summary statistics. *The Cryosphere* 6: 807-820.

Bollati I, Cerrato R, Crosa Lenz B, Vezzola L, Giaccone E, Viani C, Zanoner T, Azzoni RS, Masseroli A, Pellegrini M, Scapozza C, Zerboni A and Guglielmin M (2018) Geomorphological map of the Val Viola Pass (Italy-Switzerland). *Geografia Fisica e Dinamica Quaternaria* DOI 10.4461/GFDQ.2018.41.2

Bradley RS (ed) (2015) *Palaeoclimatology (third edition)*. London: Academic Press.

Butler DR (1995) *Zoogeomorphology: Animals as Geomorphic Agents*. Cambridge, UK: Cambridge University Press.

Butler DR (2012) The impact of climate change on patterns of zoogeomorphological influence: examples from the Rocky Mountains of the Western U.S.A. *Geomorphology* 157-158: 183–191.

Butler DR (2018) Zoogeomorphology in the Anthropocene. *Geomorphology* 303: 146–154.

Calderoni G, Guglielmin M and Tellini C (1998) Radiocarbon dating and postglacial evolution, upper Valtellina and Livignese area (Sondrio, Central Italian Alps). *Permafrost and Periglacial Processes* 9: 275 – 284.

Carturan L, Baroni C, Carton A, Cazorzi F, Fontana GD, Delpero C, Salvatore MC, Seppi R and Zanoner T (2014) Reconstructing Fluctuations of La Mare Glacier (Eastern Italian Alps) in the Late Holocene. *Geografiska Annaler: Series A, Physical Geography* 96: 287–306.

Castelletti L, Caimi R and Tremari M (2012a) Ricerche archeologiche di superficie in Val Cavargna. In: Castelletti L and Motella de Carlo S (eds) *Il fuoco e la montagna. Archeologia del paesaggio dal Neolitico all'età moderna in Alta Val Cavargna*. Como: Università degli Studi dell'Insubria, pp. 79-88.

Castelletti L, Martinelli E, Motella de Carlo S and Procacci G (2012b) Archeologia del fuoco in Val Cavargna. In: Castelletti L and Motella de Carlo S (eds) *Il fuoco e la montagna. Archeologia del paesaggio dal Neolitico all'età moderna in Alta Val Cavargna*. Como: Università degli Studi dell'Insubria, pp. 137-185.

Castelletti L and Tremari M (2012) Edifici e tracce insediative in Val Cavargna. In: Castelletti L and Motella de Carlo S (eds) *Il fuoco e la montagna. Archeologia del paesaggio dal Neolitico all'età moderna in Alta Val Cavargna*. Como: Università degli Studi dell'Insubria, pp. 89-110.

Ceriani M and Carelli M (2000) *Carta delle precipitazioni massime, medie e minime del territorio alpino della Regione Lombardia*. Milano: Servizio Geologico, Ufficio Rischi Geologici Regione Lombardia.

Colucci RR, Boccali C, Zebre M and Guglielmin M (2016) Rock glaciers, protalus ramparts and pronival ramparts in the south-eastern Alps. *Geomorphology* 269: 112–121.

Compostella C, Trombino L and Caccianiga M (2012) Late Holocene soil evolution and treeline fluctuations in the Northern Apennines. *Quaternary International* 289: 46–59.

Compostella C, Mariani GS and Trombino L (2014) Holocene environmental history at the treeline in the Northern Apennines, Italy: A micromorphological approach. *The Holocene* 24(4): 393–404.

Cornell RM and Schwertmann U (2003) *The Iron Oxides*. Weinheim: Wiley.

440 Cremaschi M and Rodolfi G (1991) *Il suolo - Pedologia nelle scienze della Terra e nella valutazione del territorio*. Roma: La Nuova Italia Scientifica.

442 Cremaschi M, Mercuri AM, Torri P, Florenzano A, Pizzi C, Marchesini M and Zerboni A (2016) Climate change versus land management in the Po Plain (Northern Italy) during the Bronze Age: New insights from the VP/VG sequence of the Terramara Santa Rosa di Poviglio. *Quaternary Science Reviews* 136: 153–172.

446 Cremaschi M and Nicosia C (2012) Sub-Boreal aggradation along the Apennine margin of the Central Po Plain: geomorphological and geoarchaeological aspects. *Geomorphologie* 2: 155–174.

448 Cremaschi M, Trombino L and Zerboni A (2018) Palaeosoils and relict soils, a systematic review. In: Stoops G, Marcelino V and Mees F (eds) *Interpretation of Micromorphological Features of Soils and Regoliths. Second edition*. Amsterdam: Elsevier, pp. 863–894.

451 Cremaschi M, Zerboni A, Nicosia C, Negrino F, Rodnight H and Spötl C (2015) Age, soil-forming processes, and archaeology of the loess deposits at the Apennine margin of the Po Plain (northern Italy). New insights from the Ghiardo area. *Quaternary International* 376: 173-188

454 Cremonese E, Gruber S, Phillips M, Pogliotti P, Boeckli L, Noetzli J, Suter C, Bodin X, Crepaz A, Kellerer-Pirklbauer A, Lang K, Letey S, Mair V, Morra di Cella U, Ravanel L, Scapozza C, Seppi R and Zischg A (2011) Brief Communication: "An inventory of permafrost evidence for the European Alps". *The Cryosphere* 5: 651-657.

458 Crosta GB, Frattini P and Agliardi F (2013) Deep seated gravitational slope deformations in the European Alps. *Tectonophysics* 605: 13–33.

460 Crouvi O, Amit R, Enzel Y, Porat N and Sandler A (2008) Sand dunes as a major proximal dust source for late Pleistocene loess in the Negev Desert, Israel. *Quaternary Research* 70: 275–282.

462 Deline P and Orombelli G (2005) Glacier fluctuations in the western Alps during the Neoglacial, as indicated by the Miage morainic amphitheatre (Mont Blanc massif, Italy). *Boreas* 34: 456-467.

464 Duchaufour P (1977) *Précis de pédologie*. Paris: Masson.

465 Duchaufour P (1983) *Pédologie. 1. Pédogenèse et classification*. Paris: Masson.

466 Dumanski JA and St-Arnaud RJ (1966) A micropedological study of eluviated horizons. *Canadian Journal of Soil Science* 46: 287–292.

468 Edwards TL, Crucifix M and Harrison SP (2007a) Using the past to constrain the future: how the palaeorecord can improve estimates of global warming. *Progress in Physical Geography* 31(5): 481–500.

471 Edwards AC, Scalenghe R and Freppaz M (2007b) Changes in the seasonal snow cover of alpine regions and its effect on soil processes: A review. *Quaternary International* 162–163: 172–181.

473 Federici PR (2005) Aspetti e problemi della glaciazione pleistocenica nelle Alpi Apuane. *Istituto*
474 *Italiano di Speleologia Mem.* 18(2): 19–32.
475 Federici PR, Ribolini A and Spagnolo M (2017) Glacial history of the Maritime Alps from the last
476 Glacial maximum to Little Ice Age. In: Hughes PD and Woodward JC (eds) *Quaternary glaciation*
477 *in Mediterranean Mountains*. London: Geological Society, Special Publications 433, pp. 137–159.
478 Fedoroff N (1997) Clay illuviation in Red Mediterranean soils. *Catena* 28: 171–189.
479 Fischer P, Hilgers A, Protze J, Kels H, Lehmkuhl F and Gerlach R (2012) Formation and
480 geochronology of Last Interglacial to Lower Weichselian loess/palaeosol sequences – case
481 studies from the Lower Rhine Embayment, Germany. *Quaternary Science Journal* 61(1): 48–63.
482 Food and Agriculture Organization (FAO) (2006) *Guidelines for Soil Description. 4th Edition*. Rome:
483 FAO.
484 Food and Agriculture Organization (FAO) (2014) *World reference base for soil resource 2014. World*
485 *Soil Resources Reports. N ° 106*. FAO, Rome: FAO.
486 Furlanetto G, Ravazzi C, Pini R, Vallè F, Brunetti M, Comolli R, Novellino MD, Garozzo L and Maggi V
487 (2018) Holocene vegetation history and quantitative climate reconstructions in a high-elevation
488 oceanic district of the Italian Alps. Evidence for a middle to late Holocene precipitation increase.
489 *Quaternary Science Reviews* 200: 212–236.
490 Gazzolo T and Pinna M (1973) *La nevosità in Italia nel quarantennio 1921-1960*. Rome: Istituto
491 Poligrafico dello Stato.
492 Giraudi C, Bodrato G, Ricci Lucchi M, Cipriani M, Villa IM, Giaccio B and Zuppi GM (2011) Middle
493 and Late Pleistocene Glaciations in the Campo Felice basin (Central Apennines - Italy).
494 *Quaternary Research* 75: 219 ‑ 230.
495 Grandi G (2012) Popolazione, attività minerarie e siderurgiche, uso dei boschi e carbonaie tra il XV e
496 il XIX secolo in Val Cavargna. In: Castelletti L and Motella de Carlo S (eds) *Il fuoco e la montagna.*
497 *Archeologia del paesaggio dal Neolitico all'età moderna in Alta Val Cavargna*. Como: Università
498 degli Studi dell'Insubria, pp. 21-36.
499 Grosjean M, Suter PJ, Trachsel M and Wanner H (2007) Ice-borne prehistoric finds in the Swiss Alps
500 reflect Holocene glacier fluctuations. *Journal of Quaternary Science* 22(3): 203–207.
501 Guzzetti F, Peruccacci S, Rossi M and Stark CP (2007) Rainfall thresholds for the initiation of
502 landslidesin central and southern Europe. *Meteorology and Atmospheric Physics* 98: 239–267.
503 Henry HAL (2007) Soil freeze–thaw cycle experiments: Trends, methodological weaknesses and
504 suggested improvements. *Soil Biology and Biochemistry* 39: 977–986.

505 Hughes PD, Woodward JC, van Calsteren PC and Thomas LE (2011) The glacial history of the Dinaric Alps, Montenegro. *Quaternary Science Reviews* 30(23–24): 3393–3412.

507 Jenny H (1941) *Factors of Soil Formation*. New York: McGraw-Hill.

508 Knight J and Harrison S (2009) Periglacial and paraglacial environments: a view from the past into the future. In: Knight J and Harrison S (eds) *Periglacial and Paraglacial Processes and Environments*. London: Geological Society, Special Publications, 320, pp. 1-4.

511 Körner C (2003) *Alpine Plant Life. Second Edition*. Berlin: Springer.

512 Kuhlemann J, Gachev E, Gikov A, Nedkov S, Krumrei I and Kubik P (2013) Glaciation in the Rila mountains (Bulgaria) during the Last Glacial Maximum, *Quaternary International* 293: 51–62.

514 Kullman L and Öberg L (2009) Post - Little Ice Age tree line rise and climate warming in the Swedish Scandes: a landscape ecological perspective. *Journal of Ecology* 97: 415–429.

516 Kutzbach JE (1976) The nature of climate and climatic variations. *Quaternary Research* 6: 471–480.

517 Loso MG, Doak DF and Anderson RS (2014) Lichenometric dating of Little Ice Age glacier moraines. *Geografiska Annaler: Series A, Physical Geography* 96: 21–41.

519 Magny M, Vannière B, Zanchetta G, Fouache E, Touchais G, Petrika L, Coussot C, Walter-Simonnet AV and Arnaud F (2009a) Possible complexity of the climatic event around 4300–3800 cal. BP in the central and western Mediterranean. *The Holocene* 19: 823–833.

522 Magny M, Peyron O, Gauthier E, Roueche Y, Bordon A, Billaud Y, Chapron E, Marguet A, Pétrequin P and Vannière B (2009b) Quantitative reconstruction of climatic variations during the Bronze and early Iron ages based on pollen and lake-level data in the NW Alps, France. *Quaternary International* 200(1-2): 102–110.

526 Mariani GS, Cremaschi M, Zerboni A, Zuccoli L and Trombino L (2018) Geomorphology of the Mt. Cusna Ridge (Northern Apennines, Italy): evolution of a Holocene landscape. *Journal of Maps* 14(2): 392-401. DOI: 10.1080/17445647.2018.1480976

529 Mariani GS, Compostella C and Trombino L (2019) Complex climate-induced changes in soil development as markers for the Little Ice Age in the Northern Apennines (Italy). *Catena* 181. DOI: 10.1016/j.catena.2019.104074

532 Mauri A, Davis BAS, Collins PM and Kaplan JO (2015) The climate of Europe during the Holocene: a gridded pollen-based reconstruction and its multi-proxy evaluation. *Quaternary Science Reviews* 112: 109–127.

535 Mayewski PA, Rohling EE, Stager JC, Karlén W, Maasch KA, Meeker LD, Meyerson EA, Gasse F, van Kreveld S, Holmgren K and Lee-Thorp J (2004) Holocene climate variability. *Quaternary Research* 62(3): 243–255.

McKeague JA, Brydon JE and Miles NM (1971) Differentiation of forms of extractable iron and aluminium in soils. *Soil Science Society of America Proceedings* 35: 33–38.

Mehra OP and Jackson ML (1960) Iron oxide removal from soils and clays by a dithionite-citrate system buffered with sodium bicarbonate. *Clays and Clay Minerals* 7: 317–327.

Munsell Color® (1994) *Munsell soil color charts*. New Windsor, NY: Munsell Color.

Murphy CP (1986) *Thin Section Preparation of Soils and Sediments*. Herts, UK: AB Academic Publishers.

Nicholson SE (1988) Land surface atmosphere interaction: physical processes and surface changes and their impact. *Progress in Physical Geography* 12(1): 36-65.

Nicolussi K (2013) Die historischen Vorstöße und Hochstände des Vernagtferners 1600-1850 AD. *Zeitschrift für Gletscherkunde und Glazialgeologie* 45-46: 9–23.

Nicolussi K, Kauffman M, Patzelt G, van der Plicht J and Thurner A (2005) Holocene tree-line variability in the Kauner valley, central Eastern Alps, indicated by dendrochronological analysis of living trees and subfossil logs. *Vegetation History and Archaeobotany* 14: 221–234.

Oliva M, Zebre M, Guglielmin M, Hughes PD, Ciner A, Vieira G, Bodin X, Andrés N, Colucci RR, Garcia-Hernandez C, Mora C, Nofre J, Palacios D, Perez-Alberti A, Ribolini A, Ruiz-Fernandez J, Sarikaya MA, Serrano E, Urdea P, Valcarcel M, Woodward JC and Yildirim C (2018) Permafrost conditions in the Mediterranean region since the Last Glaciation. *Earth Science Reviews* 185: 397 – 436.

Pelfini M, Leonelli G, Trombino L, Zerboni A, Bollati I, Merlini A, Smiraglia C and Diolaiuti C (2014) New data on glacier fluctuations during the climatic transition at ~4,000 cal. year BP from a buried log in the Forni Glacier forefield (Italian Alps). *Rend. Fis. Acc. Lincei* 25: 427–437.

Plunkett G and Swindles GT (2008) Determining the Sun's influence on Lateglacial and Holocene climates: a focus on climate response to centennial-scale solar forcing at 2800 cal. BP. *Quaternary Science Reviews* 27(1–2): 175–184.

Porter SC and Orombelli G (1985) Glacier contraction during the middle Holocene in the western Italian Alps: Evidence and implications. *Geology* 13(4): 296–298.

Regattieri E, Zanchetta G, Drysdale RN, Isola I, Hellstrom JC and Dallai L (2014) Lateglacial to Holocene trace element record (Ba, Mg, Sr) from Corchia Cave (Apuan Alps, central Italy): paleoenvironmental implications. *Journal of Quaternary Science* 29(4): 381-392.

Reimer PJ, Bard E, Bayliss A, Beck JW, Blackwell PG, Bronk Ramsey C, Buck CE, Cheng H, Edwards RL, Friedrich M, Grootes PM, Guilderson TP, Haflidason H, Hajdas I, Hatté C, Heaton TJ, Hoffmann DL, Hogg AG, Hughen KA, Kaiser KF, Kromer B, Manning SW, Niu M, Reimer RW, Richards DA, Scott EM, Southon JR, Staff RA, Turney CSM and van der Plicht J (2013) IntCal13 and Marine13 radiocarbon age calibration curves 0–50,000 years cal BP. *Radiocarbon* 55(4): 1869–1887.

Schwertmann U (1973) Use of oxalate for Fe extraction from soils. *Canadian Journal of Soil Science* 53: 244–246.

Sevink J and de Waal RW (2010) Soil and humus development in drift sands. In: Fanta J and Siepel H (eds) *Inland Drift Sand Landscapes*. Zeist, Netherlands: KNVV Publishing, pp. 107–134.

Soil Survey Staff (2014) *Keys to Soil Taxonomy. 12th ed.* Washington, DC: USDA-Natural Resources Conservation Service.

Spalla MI, Di Paola S, Gosso G, Siletto GB and Bistacchi A (2002) Mapping tectono-metamorphic histories in the Lake Como basement (Southern Alps, Italy). *Memorie di Scienze Geologiche* 54: 149-167.

Stoops G (2003) *Guidelines for analysis and description of soil and regolith thin sections*. Madison, Wisconsin: Soil Science Society of America.

Stoops G, Marcelino V and Mees F (eds) (2018) *Interpretation of Micromorphological Features of Soils and Regoliths. Second edition*. Amsterdam: Elsevier.

Van Ranst E, Wilson MA and Righi D (2018) Spodic materials. In: Stoops G, Marcelino V and Mees F (eds) *Interpretation of Micromorphological Features of Soils and Regoliths. Second edition*. Amsterdam: Elsevier, pp. 633–662.

Van Vliet-Lanoë B (1987) Dynamique périglaciaire actuelle et passée. Apport de l'étude micromorphologique et de l'expérimentation. *Bulletin A.F.E.Q*. 2: 113–132.

Van Vliet-Lanoë B (1998) Frost and soils: implications for palaeosols, palaeoclimates and stratigraphy. *Catena* 34: 157–183.

Van Vliet-Lanoë B, Coutard JP and Pissart A (1984) Structures caused by repeated freezing and thawing in various loamy sediments. A comparison of active, fossil and experimental data. *Earth Surface Processes and Landforms* 9: 553–565.

Van Vliet-Lanoë B and Fox CA (2018) Frost action. In: Stoops G, Marcelino V and Mees F (eds) *Interpretation of Micromorphological Features of Soils and Regoliths. Second edition*. Amsterdam: Elsevier, pp. 575–603.

Vepraskas MJ, Lindbo DL and Stolt MH (2018) Redoximorphic Features. In: Stoops G, Marcelino V and Mees F (eds) *Interpretation of Micromorphological Features of Soils and Regoliths. Second edition*. Amsterdam: Elsevier, pp. 425–446.

Wanner H, Solomina O, Grosjean M, Ritz SP and Jetel M (2011) Structure and origin of Holocene cold events. *Quaternary Science Reviews* 30: 3109–3123.

Waroszewski J, Egli M, Brandová D, Christl M, Kabala C, Malkiewicz M, Kierczak J, Glina B and Jezierski P (2018) Identifying slope processes over time and their imprint in soils of medium - high mountains of Central Europe (the Karkonosze Mountains, Poland). *Earth Surface Processes and Landforms* 43: 1195–1212.

Yaalon DH (1990) The relevance of soils and paleosols in interpreting past and ongoing climatic changes. *Palaeogeography Palaeoclimatology Palaeoecology* 82: 63 – 64.

Zanchetta G, Regattieri E, Isola I, Drysdale RN, Bini M, Baneschi I and Hellstrom JC (2016) The so-called "4.2 event" in the Central Mediterranean and its climatic teleconnections. *Alpine Mediterranean Quaternary* 29(1): 5 – 17.

Zerboni A, Trombino L and Cremaschi M (2011) Micromorphological approach to polycyclic pedogenesis on the Messak Settafet plateau (central Sahara): Formative processes and palaeoenvironmental significance. *Geomorphology* 125: 319-335.

Zerboni A, Trombino L, Frigerio C, Livio F, Berlusconi A, Michetti AM, Rodnight H and Spötl C (2015) The loess-palaeosol sequence at Monte Netto: a record of climate change in the Upper Pleistocene of the central Po Plain, northern Italy. *Journal of Soils and Sediments* 15: 1329–1350.

Zerboni A and Nicoll K (2018) Enhanced zoogeomorphological processes in North Africa in the human-impacted landscapes of the Anthropocene. Geomorphology 331: 22-35.

Zhang T (2005) Influence of the seasonal snow cover on the ground thermal regime: an overview. *Reviews of Geophysics* 43: RG4002.

Captions

Figure 1. (A) Hillshade of the central sector of Southern Alps indicating the location of the study area (the inset indicates its position in northern Italy). (B) Satellite view of the study area (source: Google Earth™); the star indicates the position of the soil profile.

Figure 2. (A) General view of the study area during the opening of the test trench. In the foreground the high portion of the DSGSD is visible to the right; the DSGSD is broken downslope to the left by a morphological trench associated with a counterscarp. In the background the peak of Mt. Pizzo di Gino and its southern slope are visible to the left. (B) Picture of the investigated polycyclic soil sequence indicating the position of soil horizons and samples for analyses (squares: blocks for thin sections; triangles: samples for chemical-physical analyses; dots: samples for radiocarbon dating).

Figure 3. Results of chemical-physical analyses: on the left, curves of grain size distribution (after H_2O_2 and HCl treatments); on the right, chemical determinations of Fe content. Key: Fe(o): amorphous iron; Fe(d): free iron; Fe(t): total iron.

Figure 4. Micromorphological features of the investigated soil horizons: a) well developed yellowish fabric devoid of iso-oriented features in the intermediate unit (2Bs horizon; 2x, PPL); b) depleted soil mass in the lower unit (3Et horizon; 2x, PPL); c) microlaminated clay coatings in the eluvial horizon of the lower unit (3Et horizon; 10x, PPL); d) same as c), in XPL.

Figure 5. Frost related features of the investigated soil horizons: a) horizontal planar voids in the upper unit (A2 horizon; 4x, PPL); b) groups of circular vesicles in the upper unit (A2 horizon; 10x, PPL); c) horizontal iso-oriented mica fragments in the fabric of the upper unit (Bw horizon, 10x; XPL); d) passage features produced by beetle larvae around undisturbed planar voids (A2 horizon; 4x, PPL).

Table 1. Field and chemical properties of the described soil sequence.

Table 2. Micromorphological descriptions of soil thin sections. G: gravel size; VCS: very coarse sand size; CS: coarse sand size; MS: medium sand size; FS: fine sand size; VFS: very fine sand size; S: silt size. Abundance: very dominant – >70%; dominant – 50–70%; frequent – 30–50%; common – 15–30%; few – 5–15%; very few – <5%; weak.: weakly; mod.: moderately; str.: strongly.

Table 3. Summary of microscopic properties of investigated soil horizons (full micromorphological data are in Supplementary Materials). Frost related pedofeatures in *italics*.

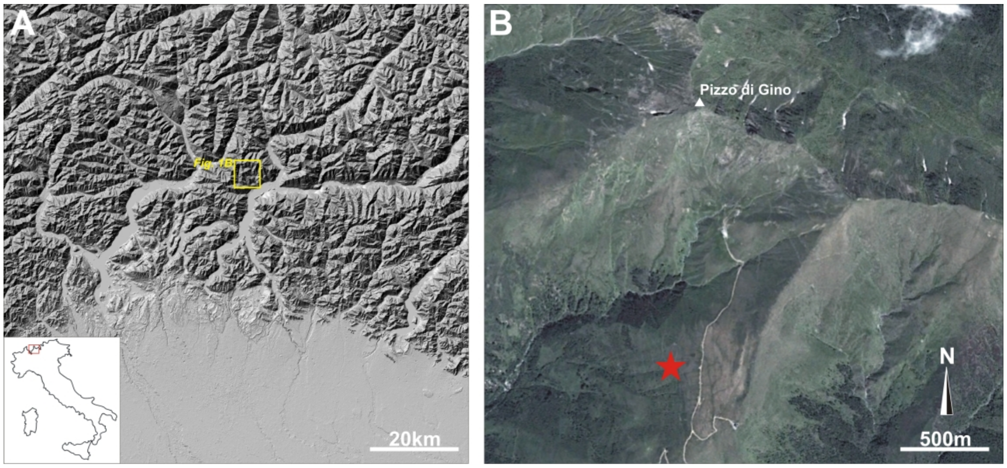
A
Fig. 1B
20km
B
Pizzo di Gino
N
500m


A
B
O
A1
A2
Bw
2E
2Bs
2BC
3Et
3Bs
3C
2683±42
2730±43
6850±20

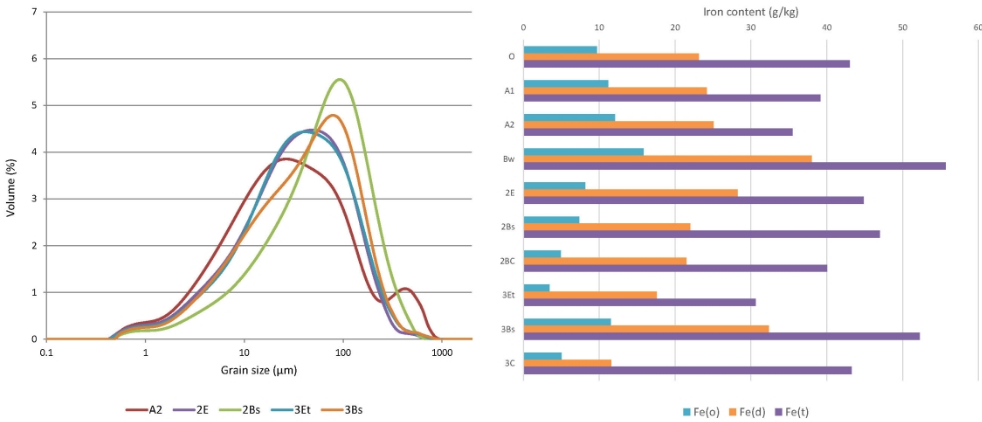

337x150mm (200 x 200 DPI)

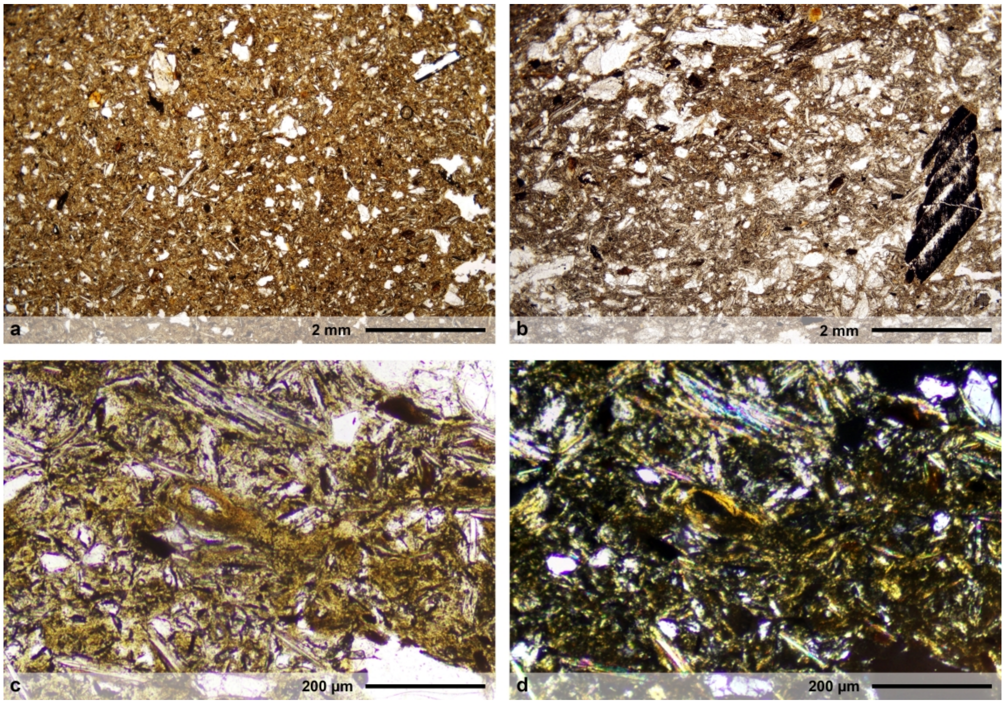

420x292mm (300 x 300 DPI)

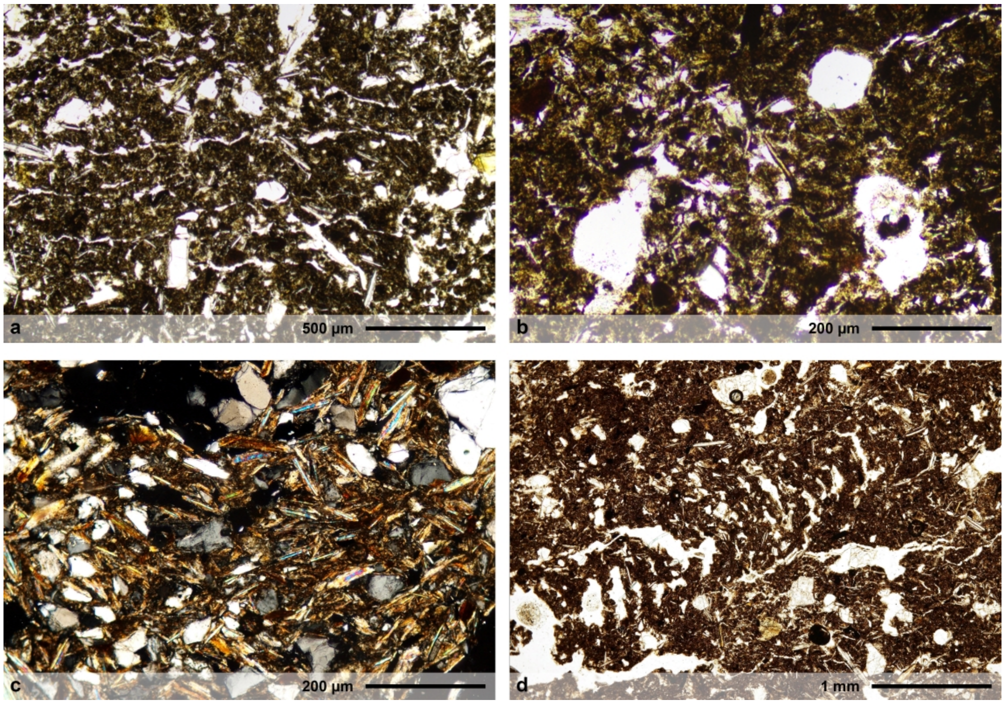

420x292mm (300 x 300 DPI)

Horizon	Texture	Colour	Mottles	Fe(o) (g/kg)	Fe(d) (g/kg)	Fe(t) (g/kg)
O	Silty loam	10YR 3/2		9.67	23.14	43.03
A1	silty loam	10YR 3/2	10 YR 6/6	11.18	24.20	39.17
A2	silty clay	10YR 2/1		12.06	25.05	35.51
Bw	silty loam	10YR 6/8		15.86	38.02	55.66
2E	silty clay	10YR 5/4		8.16	28.26	44.88
2Bs	silty sand	10YR 5/6		7.36	22.00	47.02
2BC	silty sand	10YR 6/4		4.90	21.47	40.06
3Et	silty clay	10YR 6/1	10YR 6/8, 5Y 5/8	3.44	17.55	30.61
3Bs	silty clay	10YR 5/8		11.53	32.37	52.27
3C	silty sand	10YR 4/2		5.00	11.59	43.30

Horizon	Microstructure	Aggregates	Porosity
A1	Crumb	Dominant weak. separated crumbs, FS to VFS; dominant weak. separated granular peds inside crumbs, SS	Common complex packing voids, MS to SS; very few linear planes locally horizontally oriented, MS to SS; very few channels, VCS to CS; very few vughs, MS to FS; ; very few vesicles, FS to VFS
A2	Granular	Dominant weak. separated granular peds, SS	Very few complex packing voids, FS to VFS; few linear planes horizontally oriented, MS to VFS; few channels, CS to FS; very few vughs, MS to FS; very few vesicles, FS to VFS
Bw	Channel	Dominant weak. separated granular peds, SS	Common channels, CS to FS; few vughs, MS to FS
2E	Channel	No visible aggregates	Few channels, CS to FS; very few vughs, MS to FS
Fireplace	Channel	Few weak. separated granular peds, SS	Common channels, CS to FS; few vughs, MS to FS
3Et	Complex, vughy/spongy	No visible aggregates	Very few channels, CS to FS; few vughs, CS to FS
3Bs	Channel	Frequent weak. separated granular peds, SS	Few channels, CS to MS; few vughs, MS to FS; very few complex packing voids, FS to VFS

G: gravel size; VCS: very coarse sand size; CS: coarse sand size; MS: medium sand size; FS: fine sand siz moderately; str.: strongly.

Mineral fragments	Organic material	c/f limit, ratio	c/f related distribution
Common weak. weathered micas, CS to VFS, well sorted on FS; few weak. weathered FS quartz and feldspar, MS to VFS; very few mod. weathered rock fragments, GS to CS	Very few charcoal fragments, GS to MS; very few plant remains (roots), GS to CS	10 µm, 60/40	Single spaced porphyric
Few weak. weathered micas locally sub-horizontally oriented, FS to VFS; very few weak. weathered FS quartz and feldspar, FS to VFS; very few mod. weathered rock fragments, GS to CS (GS concentration on the upper boundary with A2)	Very few charcoal fragments, CS to FS; very few plant remains (roots), VCS to CS	10 µm, 40/60	Double spaced porphyric
Common weak. weathered micas locally sub-horizontally oriented, MS to VFS; few weak. weathered FS quartz and feldspar, MS to FS; very few mod. weathered rock fragments, VCS to CS	Very few charcoal fragments, CS to FS; very few plant remains (roots), CS to MS	10 µm, 75/25	Close porphyric
Common weak. weathered micas, MS to VFS; very few weak. weathered FS quartz and feldspar, MS to FS; very few mod. weathered rock fragments, VCS to CS	Very few charcoal fragments, CS to FS; very few plant remains (roots), CS to MS	10 µm, 75/25	Close porphyric
Common weak. weathered micas, MS to VFS; few weak. weathered FS quartz and feldspar, MS to FS; very few mod. weathered rock fragments, VCS to CS	Frequent charcoal fragments, GS to MS; very few plant remains (roots), CS to MS	10 µm, 75/25	Close porphyric
Frequent weak. weathered micas, MS to VFS; few weak. weathered FS quartz and feldspar, CS to FS; few mod. weathered rock fragments, GS to CS	Very few charcoal fragments, VCS to MS	10 µm, 80/20	Close porphyric
Common mod. weathered micas, CS to VFS; few weak. weathered FS quartz and feldspar, MS to VFS; few mod. weathered rock fragments, GS to CS	Very few charcoal fragments, MS to FS	10 µm, 40/60	Single spaced porphyric

ze; VFS: very fine sand size; S: silt size. Abundance: very dominant – >70%; dominant – 50–70%; frequen

FS material	b-fabric	Pedofeatures
Brown (darker with depth) dotted	Undifferentiated, dark brown	Very few subangular alteromorphic Fe-Mn nodules with sharp boundary, CS to FS; very few rounded typic Fe-Mn nodules with clear boundary, FS to SS; very few dense incomplete matrix infillings (passage features), GS to VCS
Dark brown dotted	Undifferentiated, dark brown	Very few subangular alteromorphic Fe-Mn nodules with sharp boundary, CS to FS; very few rounded typic Fe-Mn nodules with clear boundary, FS to SS; very few dense incomplete matrix infillings (passage features), GS to CS
Yellowish brown speckled	Stipple speckled, brown	Very few subangular alteromorphic Fe-Mn nodules with sharp boundary, VCS to FS; very few rounded typic Fe-Mn nodules with clear boundary, MS to SS; very few dense incomplete matrix infillings (passage features), GS to CS
Grayish brown speckled	Stipple speckled, grayish brown	Very few subangular alteromorphic Fe-Mn nodules with sharp boundary, VCS to FS; very few rounded typic Fe-Mn nodules with clear boundary, MS to SS; very few dense incomplete matrix infillings (passage features), GS to CS
Yellowish brown speckled	Stipple speckled, brown	Very few subangular alteromorphic Fe-Mn nodules with sharp boundary, VCS to FS; very few rounded typic Fe-Mn nodules with clear boundary, MS to SS; very few dense incomplete matrix infillings (passage features), GS to CS
Gray speckled	Crystallitic, gray	Very few subangular alteromorphic Fe-Mn nodules with sharp boundary, VCS to FS; very few microlaminated typic-crescent dusty clay coatings VFS to SS; very few fabric hypocoatings (compaction) around channels
Reddish brown speckled	Stipple speckled, reddish brown	Very few subangular alteromorphic Fe-Mn nodules with sharp boundary, VCS to MS; very few rounded typic Fe-Mn nodules with clear boundary, MS to VFS

nt – 30–50%; common – 15–30%; few – 5–15%; very few – <5%; weak.: weakly; mod.:

Horizon	Microstructure	Aggregates	Porosity
A1	Crumb	Dominant granular	Complex packing voids, linear planes locally horizontally oriented, vesicles
A2	Granular	Dominant granular	Channels, linear planes locally horizontally oriented, vesicles
Bw	Channel	Dominant granular	Channels, vughs
2E	Channel	None	Channels, vughs
Fireplace	Channel	Few granular	Channels, vughs
3Et	Vughy/spongy	None	Channels, vughs
3Bs	Channel	Frequent granular	Channels, vughs, complex packing voids

Mineral fragments	Charcoal fragments	c/f ratio	c/f related distribution	Fine material
Common micas, few quartz and feldspar, very few rock fragments	Very few	60/40	Single spaced porphyric	Brown
Few micas horizontally oriented, very few quartz and feldspar, very few rock fragments	Very few	40/60	Double spaced porphyric	Dark brown
Common micas horizontally oriented, few quartz and feldspar, very few rock fragments	Very few	75/25	Close porphyric	Yellowish brown
Common micas, very few quartz and feldspar, very few rock fragments	Very few	75/25	Close porphyric	Grayish brown
Common micas, few quartz and feldspar, very few rock fragments	Frequent	75/25	Close porphyric	Yellowish brown
Frequent micas, few quartz and feldspar, few rock fragments	Very few	80/20	Close porphyric	Gray
Common micas, few quartz and feldspar, few rock fragments	Very few	40/60	Single spaced porphyric	Reddish brown

b-fabric	Pedofeatures
Undifferentiated	Fe-Mn nodules, passage features
Undifferentiated	Fe-Mn nodules, passage features
Stipple speckled	Fe-Mn nodules, passage features
Stipple speckled	Fe-Mn nodules, passage features
Stipple speckled	Fe-Mn nodules, passage features
Crystallitic	Fe-Mn nodules, passage features, dusty clay coatings
Stipple speckled	Fe-Mn nodules

Was the Little Ice Age the coolest Holocene climatic period in the Italian central Alps?

Abstract

Estimation~~s~~ of the relative intensity of different cold periods occurring during ~~of~~ the Late Quaternary are difficult tasks, particularly in non-glaciated mountain landscapes, and where high- to medium-resolution archives for proxy data are lacking. In this paper, we study a Holocene polycyclic soil sequence in the central Alps (Val Cavargna, Northern Italy)~~explore an alternative tool – soil micropedology –~~ to estimate climatic parameters (specifically T) changes in non-glaciated, high altitude environments. ~~A Holocene polycyclic soil sequence in the central Alps (Val Cavargna, Northern Italy)~~ W~~w~~e investigate this key site ~~was investigated~~ through palaeopedological and micromorphological analyses in order to understand phases of soil development ~~its formation~~ and detect hidden evidence of cold conditions during its formation. Three phases of pedogenesis ~~could~~ can be recognized and attributed in time to different periods during ~~of~~ the Holocene. Pedogenetic phases were separated by two truncation and deposition episodes~~s~~ related to the reactivation of slope processes under cold conditions at the onset of the Neoglacial and the Iron Age Cold Epoch (IACE) respectively. ~~Robust~~ Micromorphological evidence~~s~~ ~~stress evidence of~~ of frost action on soil ~~revealed by micropedology could~~ can instead relate to pedogenetic processes acting in the Little Ice Age (LIA). The different expression of these three cold periods corresponds to different climatic conditions, pointing to the LIA as a cooler/drier period in comparison to the preceding ones.

Keywords

Polycyclic palaeosols; Micropedology; Frost pedofeatures; Mid-Late Holocene; Little Ice Age; Southern Alps.

I. Introduction

One of the most difficult tasks in paleoclimate past climate studies – before the introduction of instrumental measurements – is the estimation , even relative, of climate parameters and their variation with across time (Edwards et al., 2007a; Bradley, 2015). When records are irregular and limited to shortened time-spans, discontinuous or low in resolution, such as in many continental palaeoenvironmental archives, the reconstruction of climatic conditions and their effects on the landscape becomes much more challenging (Kutzbach, 1976; Federici, 2005; Giraudi et al., 2011; Bradley, 2015; Furlanetto et al., 2018). This is especially true when dealing with the effects of cold periods in middle latitude and Mediterranean mountain ranges, such as the Alps and Apennines of Italy, known as highly dynamic regions (Porter and Orombelli 1985; Baroni and Orombelli 1996; Federici, 2005; Hughes et al., 2011; Kuhlemann et al., 2013; Pelfini et al., 2014; Colucci et al., 2016; Bollati et al., 2018). Where extensive landforms and stratigraphic records of Quaternary glacial advances are not present, evident traces of cold phases are often hard to study. Poorly visible, buried and hidden signs of cold periods – as much as of the subsequent warm phases – are only occasionally embedded and rarely well-preserved in landforms and within (palaeo)soilssols and sedimentary records (Angelucci et al., 1992; Calderoni et al., 1998; Fischer et al., 2012; Compostella et al., 2012, 2014; Waroszewski et al., 2018). In the latter, evidence of cold phases is often associated with breaks in the sedimentary succession or with an increased frequency of slope processes related to climatic instability (Bertolini et al., 2004; Nicolussi et al., 2005; Magny et al., 2009a; Arnaud et al., 2012; Cremaschi and Nicosia, 2012; Compostella et al., 2014; Pelfini et al, 2014; Mariani et al., 2019). Despite the extensive documentation regarding on the Little Ice Age (LIA) traced in paleoclimate studies (Kullman and Öberg, 2009; Arnaud et al., 2012; Nicolussi, 2013; Carturan et al., 2014; Loso et al., 2014), many questions are still open, for example its role and importance inside the wider frame of the Holocene is less understood. For instance, LIA's the influence of climate variations on non-glaciated mountain landscapes during the LIA is poorly known, especially when compared to previous older cold intervals such as the Neoglacial, the Lateglacial, and the Last Glacial Maximum (LGM) (e.g., Wanner et al., 2011; Badino et al., 2018; Furlanetto et al., 2018). In the mountain environments of middle latitudes, where glacial and periglacial landforms are undetectable or have been vanished/truncated/ erased due to enhanced slope activity (e.g.: Allison, 1996; Giraudi et al., 2011; Compostella et al., 2014; Mariani et al., 2018), paraglacial (Knight and Harrison, 2009), or zoogeomorphological processes (e.g., Butler, 1995, 2012), the effects of cold phases are virtually absent from the scientific record.

In this paper, we studied ~~consider~~ a Holocene polycyclic soil sequence formed in the Mid-Late Holocene in the Italian Central Alps (Val Cavargna, CO). Our aim is to find records ~~ways to detect hidden evidence~~ of Holocene climatic influence on the evolution of surface processes (Nicholson, 1988), and to assess whether soils and paleoso~~i~~ils (and their pedofeatures) can ~~really~~ record climatic changes in Alpine environments. The studied ~~considered~~ soil sequence shows clear traces of the presence of cold conditions during its formation, strong enough to promote soil frost and trigger the formation of frost-induced pedofeatures (*sensu* Van Vliet-Lanoë, 1998; Van Vliet-Lanoë et al., 2018) without the influence of glacial or periglacial processes. No evidence for glacials ~~landforms,~~ were found at the study site and in its close ~~not present in the~~ vicinity. ~~– of the study site~~. Using multiple palaeopedological techniques, and in particular micropedology, we were ~~are~~ able to characterize different Holocene cold phases ~~eriods~~ affecting ~~acting on the~~ soil formation. We also stress ~~also suggest interpretations on the relative intensity~~ the impact as a climatic parameter of ~~of~~different atmospheric temperatures ~~–~~ during the cold periods of the last few millennia.~~and its impact as a climatic parameter during the last few millennia.~~ We lastly suggest ~~offer~~ an alternative qualitative approach to interpret past fluctuations of climatic parameters based on their effect on surface processes.

II. The study area

The studied soil sequence is located at Alpe Piazza Vacchera (46°06′32′′N, 9°08′33′′E), in Val Cavargna (San Bartolomeo municipality, Italian Central Alps), at an elevation of 1680 m a.s.l. (Figures 1 and 2). The bedrock of the studied area is part of ~~belongs to~~ a portion of the Southalpine basement – the tectono-metamorphic unit of the Dervio–Olgiasca Zone (after Spalla et al., 2002) – and consists mainly of garnet-staurolite-bearing schist and minor gneiss with lenses of amphibolite. Schists are particularly prone to weathering, especially in areas of pervasive jointing due to tectonic deformation. The study site is currently above the treeline and covered by grassland pastures; mean annual rainfall is between 2000–2500 mm/y and mean annual temperature between 3.8 and 10.9°C (Ceriani and Carelli, 2000). Snow accumulation is high, estimated between 1–2 m/y, with a residence time ~~higher~~ greater than 100 days (Gazzolo and Pinna, 1973). The permanent snow line for the Alps varies from N to S and from W to E according to factors related to latitude, continentality and slope insulation, but it is generally located between 2500–2800 m a.s.l. (Barry, 1992), thus well above the area of study. The area ~~is with no~~ does not contain ~~unaffected by the presence of~~ permafrost: in this portion of the Alps favourable conditions for permafrost ~~is~~are found only ~~formation can only be met~~ above 2200–2300 m a.s.l. (Boeckli et al., 2012), and the first instances of permafrost or related landforms are found in a range of tens~~?~~ of ~~many~~ kilometres to the North (Cremonese et al., 2011). During the LGM, valley glaciers did not cover the area but at least a few cirque or slope glaciers were present in the highest part of the mountain~~ous~~ range ~~region~~ (Bini et al., 2009). Since then, no traces of further glacial influence are found on the slopes or in the valley below (Bini et al., 2009). Periglacial processes are visible as sparse, possibly inactive solifluction lobes on the surrounding slopes, today highly disturbed by zoogeomorphologically induced game trails, causing ~~—~~ ~~and related~~ instability~~,~~ and ~~causing~~ enhanced gully erosion and transportation of soil material in the vicinity of the studied area (e.g., Butler, 2018; Zerboni and Nicoll, 2018).

Human ~~frequentation~~ activity in Val Cavargna is known since the Mesolithic, with the establishment and abandonment of sporadic settlements in the upper part of the valley. Subsequent occasional occupation of the area with evidence of widespread forest fires took place multiple times from the Neolithic to the Middle Ages (Castelletti et al., 2012a). The systematic exploitation of the area, resulting in an increase in human pressure on the landscape, dates back mainly to post-medieval times (Castelletti and Tremari, 2012). Documented instances of forest clearance in the upper valley appear since the XVI century CE, with a change in land use for charcoal production (Grandi, 2012). At this time, large portions of deforested land – between 1400-1800 m a.s.l. – were converted to pasture lands (Castelletti et al., 2012b). Near the studied section, the first establishment of a small cattle farm and trail can be loosely attributed to the same period.

III. Materials and methods

To investigate the soil in the field we dug a trench along the western slope of Mount Pianchette – Pizzo di Gino, in correspondence of a natural filled trench forming a small terrace on a deep-seated gravitational slope deformation (DSGSD). This landform represents large to extremely large mass movements generally affecting the entire length of high-relief valley flanks, extending up to 200–300 m in depth, which can frequently extend beyond the slope ridge (Crosta et al., 2013). Soil descriptions and horizon designations were carried out according to the guidelines of FAO (2006); colour definition followed the Munsell Color® (1994) nomenclature. The diagnostic horizons of buried palaeosols in the sequence were defined according to the international classification systems (FAO, 2014; Soil Survey Staff, 2014; Zerboni et al., 2011, 2015). Soil samples for chemical-physical analyses were collected for each horizon. Particle size distribution was determined using laser diffraction (Malvern Mastersizer MS-2000) after H_2O_2 and HCl treatments, according to the procedure described in Crouvi et al. (2008). The total amount of Fe and Al in the samples was determined by complete dissolution in a mixture of HF, HCl, HNO_3 and $HClO_4$, followed by measurement of the solubilised ions using an ICP-ES (Jobin-Yvon JV24). Dithionite- (Mehra and Jackson, 1960) and oxalate-extractable (McKeague et al., 1971; Schwertmann, 1973) fractions of Fe and Al oxyhydroxides, representing a quantification for free and amorphous Fe and Al forms respectively, were also measured with the same instrument. The Activity Ratio between oxalate- and dithionite-extractable iron (Fe(o)/Fe(d)) was also calculated. Analytical data are reported in Table 1 and summarized in Figure 3.

Thin sections were produced from undisturbed samples taken from relevant soil horizons after impregnation with polyester resin according to the method described in Murphy (1986). Slides were examined with an Olympus BX41 petrographic microscope, under plane-polarized light (PPL), cross-polarized light (XPL), and oblique incident light (OIL). The terminology of Stoops (2003) was used to describe thin sections, whereas micromorphological interpretation was mainly based on the concepts reported in Stoops et al. (2018).

The age of the polycyclic soil sequence was obtained by dating with radiocarbon (AMS-^{14}C) two samples of charcoal. AMS-^{14}C dating results were calibrated (2σ range) using the INTCAL13 curve (Reimer et al., 2013).

IV. Results

Along the slope of Mt. Pianchette and Mt. Pizzo di Gino, inside the morphological trench formed by a detachment niche of a DSGSD, are present a series of shallow depressions ~~allowed several events of accumulation of poorly sorted sediments after colluvial phenomena and slope processes, later weathered into soils.~~filled with sediments deposited through colluvial slope processes that were subsequently weathered and reorganized into soils. In the uppermost depression, several soil horizons were identified (Table 1), consisting of three different soil units on successively deposed parent materials (Figure 2). The uppermost unit corresponds to the extant soil, down to a depth of about 49 cm. It is an organic temperate mountain soil differentiated in thicker organic A horizons sometimes alternated with thinner levels of rubified soil material containing dark mottles. The same material is also present at the bottom of the unit as a mineral Bw horizon. The ~~passage~~ boundary between this unit and the intermediate one is marked by an erosional surface bearing a residual lens of macroscopic charcoal fragments, several centimetres thick, identified as the remains of a fireplace. Dating from two charcoal samples taken from this lens gave a result of 2730±43 (RC-369) and 2683±42 (RC-370) years uncal BP (2926–2756 years cal BP and 2863–2747 years cal BP respectively). The intermediate unit is a buried palaeosol divided into three main horizons: an eluvial 2E horizon occupies the upper position above a rubified 2Bs horizon; below them is ~~found~~ a mineral 2BC horizon with common reddish mottles. The lowermost soil unit, starting at a depth of 75 cm, is quite similar to the previous one, but pedofeatures are better expressed. A whitish eluvial 3Et horizon, in which are still present reddish mottles comparable to those of the level above it, forms the upper portion of the unit, followed by a weathered rubified 3Bs horizon. Below the latter, a 3C horizon marks the ~~passage~~ boundary to the bedrock at about 130 cm below the current surface. Charcoal fragments from the 3Bs horizon of this unit were dated to 6850±20 years uncal BP (UGAMS-38048, 7721–7621 years cal BP).

Grain size analytical data from a selection of soil samples shows where units differ and where instead similarities emerge (Figure 3). The A2 horizon of the top unit differs ~~stands out~~ from the others, showing a bimodal distribution of grain size classes: the main mode is represented by silt, while a secondary mode is ~~instead~~ shifted towards medium/coarse sand. Its much broader ~~selection~~ distribution also indicates a poor selection of grains. Horizons from the other two units show ~~instead~~ very similar categories. In particular, the E horizons share almost the same bell curve weakly skewed to the left and centred on coarse silt. All B horizons (Bw, 2Bs and 3Bs) also share a similar trend with a ~~better selected~~ mode at ~~into~~ the fine sand and a higher skewness towards the finer fractions that are more expressed in the bottom unit. Total iron content in the soil sequence amounts to 3-5.5% of the total mass in all soil horizons, with concentrations in the B horizons of the top and bottom units (Figure 3; Table 1). Eluvial horizons show lower concentrations of Fe, with the 3Et horizon being the scarcest in total iron content (3.06%). The intermediate unit is also low in iron content, with only a slight increase of total iron in the 2B horizon. Free iron measured as Fe-dithionite peaks in the Bw and 3B horizons and shows the lowest concentration at the bottom of the sequence (11.6 g/kg in the 3C horizon); generally, free iron accounts for 47-71% of total iron content. The Activity Ratio is mostly between 0.35 and 0.5 for all horizons, with the exception of E horizons where it reaches the lowest values (below 0.3).

The observation of thin sections reveals the general composition and fabric of the soil units (Table 2). The micromass of all investigated horizons shows a dominance of coarse mineral material (mainly micas, then quartz and feldspar) with the fine material either compactly filling the remaining space in B horizons (Figure 4a), or weakly aggregating in granular peds in E horizons (Figure 4b). Fine charcoal is always present; coarser fragments can be found in the A1 and 3Et horizons as well as in the charcoal-bearing lens at the top of the 2E horizon. The 3Et horizon shows microlaminated clay coatings (Figure 4c, d) inside a groundmass with marked differences from the B horizons: the fine material bears a greyish colour and no visible aggregation is present. The A1 and A2 horizons are locally arranged in a pattern of horizontal planar voids (isoband fabric, *sensu* Dumanski and St-Arnaud, 1966), not visible in the deeper parts of the soil sequence (Figure 5a). This pattern is randomly distributed in the two horizons as large centimetric patches sharing the same features: a net of partially interconnected straight or slightly curved planar voids up to a millimetre long and less than 100 μm thick that separate lenses of soil material up to 1 mm thick. Vesicles are often associated ~~to~~ with soil lenses (Figure 5b) and the pattern itself. Clusters of parallel-oriented coarse fragments (Figure 5c) are visible in the Bw horizon. All these features are usually undisturbed by the presence of bioturbation otherwise found in many instances in the soil mass in the form of passage features (Figure 5d).

V. Discussion

In the following parts we reconstruct the evolution of the investigated soil sequence discussing the main pedogenetic processes involved in its formation. We then highlight the occurrence of pedofeatures in the different soil units that record ~~allow the reconstruction of~~ past temperature shifts in the area.

5.1. Soil forming processes and chronology

The characterization of pedogenesis in the three units shows evidence of similar soil formation processes in different periods of time, thus confirming the existence of a soil polysequence (Cremaschi and Rodolfi, 1991). The very similar grain sizes of the different horizons imply that each soil unit was formed by deposition over the previous surface – exposed by truncation – of the same type of sediments removed from above by short-range (tens to hundreds of metres) slope transportation~~?~~ movements. Each soil unit shares the combined presence of an E/B horizon series, with the E substituted by a moderately depleted A2 horizon in the uppermost unit. The formation of clay and Fe oxyhydroxides in the soil mass is accompanied by their translocation downwards from the eluvial horizons into the lower rubified B horizons, or even below in older soil units, as in the case of the clay coatings ~~found inside~~that crossed the boundary into the 3Et horizon. Particle translocation is also supported by the ~~highlighted by the~~ shift from the 2Bs to the 3Et horizon, which hints to clay depletion from the second unit and illuviation into the unit ~~one~~ below, ~~. An~~ and by the enrichment in fine material ~~is also clearly visible~~ in the 3Bs horizon. The low activity ratio ~~also weakly~~ shows ~~highlights this trend showing~~ a relative depletion in the amorphous iron forms, easier to mobilise, in E horizons. The three units show different degrees of the same pedogenetic processes ~~(~~pedoplasmation, soil formation by weathering and translocation of clay minerals and Fe

Commented [RA1]: The discussion is too long and you lose focus. If you can shorten it a bit and make it tighter, it will be great .

All in the light of your main conclusion " Our study show new evidence regarding the importance of the LIA in the Alps as one of the main cold intervals after the LGM".

Commented [a2]: Secondo me qui non c'è nulla da fare….

oxyhydroxides; Duchaufour, 1983), decreasing in strength of expression upwards. In fact, although the bottom unit looks the most developed in a well-defined series of horizons, Fe oxyhydroxides do not change ~~sensibly~~ markedly along the units, showing again uniformity in weathering. Pedogenesis is in any case only moderately developed, and the accumulation of Fe in the B horizons appears to be not only a result of in-situ weathering ~~alone~~, but also of translocation from the overlying horizons and younger parent materials (Duchaufour, 1977; Cornell and Schwertmann, 2003).

Pedogenesis occurred under warm/temperate climate phases with the presence of continuous vegetation (Duchaufour, 1983) ~~that~~ and promoted the accumulation of microlaminated clay coatings by illuviation into the unit below (e.g. Fedoroff, 1997; Compostella et al., 2014). The microstructure of E horizons and the presence of red mottles in B horizons (Table 3) suggest an incipient podsolization process (Duchaufour, 1983; Van Ranst et al., 2018), likely supported ~~helped~~ by local conditions of seasonal~~ly ?periodical~~ water saturation (Duchaufour, 1983; Sevink and de Waal, 2010; Vepraskas et al., 2018). The identification of wood species from charcoal fragments found in various soil horizons shows the dominance of silver fir (*Abies alba*) ~~open forest~~ throughout the soil sequence~~;~~, reconstructions of the vegetation history of the area point to the presence of an open forest ~~indicating~~ under moderately warm conditions (Castelletti et al., 2012b). At the current surface and towards the top of the intermediate unit, charcoal assemblages suggest a sparsely forested heathland, revealing colder phases of forest retreat or anthropogenic pressure (Castelletti et al., 2012b).

Radiocarbon dating stresses– ~~helps in placing the~~ formation of the various soil units within the Holocene, showing how the soil sequence has in fact experienced more than one warm climate phase. The development of the bottom unit, dated to 7721–7621 years cal BP, can be very clearly attributed to the Early-Middle Holocene (Mayewski et al., 2004; Arnaud et al., 2012; Grosjean et al., 2007), during a warm period preceding the cold event at 4.2 ka cal BP (e.g., Zanchetta et al., 2016), possibly the Atlantic Warm Period (AWP) or the Late Neolithic Thermal Maximum (LNTM). In this longer period of pedogenesis, potentially lasting a few thousands of years, the soil had the time to develop pedofeatures under a rapidly warming phase~~climate~~. Afterwards, the warm and stable phase responsible for the formation of the intermediate unit should occur after the Middle/Late Holocene transition, when several warm fluctuations occurred (Mayewski et al., 2004; Deline and Orombelli, 2005): the longest phase takes place during the Bronze Age, loosely between 3800 and 2800 years BP (e.g., Arnaud et al., 2012 and references therein), and can be confirmed by dating from the truncation of the unit indicated by the residual fireplace (2926–2756 and 2863–2747 years cal BP). It is therefore possible that this pedogenesis took place in a period not much longer than a thousand years. The truncation points to the transition ~~passage~~ from a warm period to the next cold phase (Plunkett and Swindles, 2008; Magny et al., 2009b; Wanner et a., 2011; Regattieri et al., 2014; Cremaschi et al., 2016) corresponding to the Iron Age Cold Epoch (IACE). This cold stage probably witnesses both the truncation of the intermediate unit due to enhanced slope processes and the deposition of the parent material composing the top one. The last phase of pedogenesis probably started since the Roman Warm Period (RWP) onwards to present time, covering less than 2000 years of duration in a fluctuating climate.

5.2. Are frost-related pedofeatures a proxy for past temperatures?

The typical pedofeatures found at ~~in~~ the top unit (A1-A2 horizons) relate to specific climate conditions and can be safely attributed to a post-RWP cold ~~ol~~ phase on the basis of the above-mentioned chronological framework. The LIA is most likely the ~~coolest~~ coldest ~~–~~ climatic phase in that time interval (Wanner et al., 2011; Furlanetto et al., 2018). The pattern of microscopic horizontal planar voids separating the matrix into?? ~~Dividing~~ homogeneous lenses of soil material indicates the action of frost on soil horizons (Dumanski and St-Arnaud, 1966). Vesicles are also related to the entrapment of air bubbles in the soil mass during the freezing process (Table 3). As suggested by Van Vliet-Lanoë (1987, 1998) and Van Vliet-Lanoë et al. (2018), this regular pattern is connected to the presence of intermittent or seasonal frost episodes localised at the soil surface when the penetration of the freezing front is not very deep. This is expected for temperate environments, considering that very low air temperatures are needed to freeze the open ground below the first centimetres (Henry, 2007). Deformation of the soil mass is only limited to sporadic preferential orientations of coarse fragments, also indicating weak freezing conditions (Van Vliet-Lanoë et al., 1984). Nevertheless, the durability of these features to later pedo/bio-turbation (Van Vliet-Lanoë et al., 1984) indicates a certain level of stability compatible with repeated freeze-thaw cycles during an extended period.

The weak expression of the above described frost-related pedofeatures suggests the occurrence in the past of periglacial processes unrelated to permafrost (Van Vliet-Lanoë, 1998), the presence of which would have forced much stronger cryoturbation and very different features in the soil and is linked to more rigid conditions, possibly unmet here since the LGM. In fact, considering the stability through time of frost-related pedofeatures (Van Vliet-Lanoë et al., 1984), their absence in the two buried soil units suggests that frost acted in the area only ~~in recent times~~during the most recent cold phase corresponding to the LIA, after the accumulation of the parent material of the uppermost soil unit. Since most of the pedogenetic factors identified by Jenny (1941) and the related soil-forming processes do not show dramatic changes over time, as seen above, this occurrence is probably more related to fluctuations ~~modifications~~ in the climate. A climatic trend toward cooler conditions seems also confirmed by the general decrease in expression of pedogenetic processes from the bottom to the top of the pedosequence. This trend has been recently suggested from multi-proxy models of insolation at middle latitudes on alpine scale (Mauri et al., 2015). The supposed duration for each phase of soil formation, probably lasting several millennia to centuries, also needs to be taken into consideration. It is clear how time alone is not able to explain the differences in pedogenesis. In fact, both factors contributed in synergy to the development of soil formation processes (~~Jenny, 1941~~Boardman, 1985; Birkeland, 1999). We believe that in this case, while no simple comparison can be done between climate and time, the former seems to play the main role. The rapid succession of environmental changes in ~~the environmental conditions during~~ the Holocene represents the limiting factor in the development of pedogenesis.~~;~~ ~~while In fact, the amount of time, though necessary for soil formation, is more relevant as the duration of the climate phases than as a factor itself.~~Time in this case cannot be the primary factor driving the expression of pedogenesis, since the different units are formed too suddenly because of the continuous climate shifts.

Considering the strong similarities in soil formation conditions between the three units, the effect of different cold periods on each is very noticeable. The abrupt truncation of the bottom unit could possibly correspond to the initial part of the Neoglacial period, often associated with a sharp increase in denudation processes (Arnaud et al., 2012). Denudation is in turn related to vegetation loss events often indirectly caused by the passage to cold and unstable climate phases (Bertolini et al., 2004; Nicolussi et al., 2005; Magny et al., 2009a; Compostella et al., 2014). Slope instability events responsible for the deposition of the two upper units are also a typical result of denudation processes, where erosion and deposition often occur consecutively on the same topographic surface (Giraudi et al., 2011; Compostella et al., 2014). The same appears to happen for the truncation of the second unit dated to the IACE (Magny et al., 2009b). For sake of clarity we need to consider that the anthropogenic contribution to the deposition and development of these units is not to be underestimated. Multiple fire events very likely connected to forest clearance practices started in the area since the Mesolithic (Castelletti et al., 2012b). Fire events greatly enhanced the effect of washout and solifluction on the slopes, mobilising the colluvial material that forms the two upper soil units. Human contribution to slope instability is in this case quite important, enhancing ongoing processes in synergy with the effect of climate variations. Later, also the zoogeomorphological effect due to the introduction of herding may have contributed to accelerate ongoing denudation and rill erosion.

The different setting of the uppermost unit, where frost features represent the effect of cold conditions in place of truncations, can be ultimately regarded as a distinct process attributed specifically to the LIA. Neoglacial cold events appear to have mainly impacted the soil through slope instability and processes of removal/addition of material, but no features directly related to freezing and ice formation are found ~~on the surface~~at the top of the buried units. In this regard, while it is true that no actual surface A horizon is currently present on both units, it must be noted that the new surfaces produced by truncation were probably exposed to the weather for a non-insignificant length of time. On the intermediate unit this was enough to allow the establishment of a fireplace on top of the former topographic surface - or at least not far from it – which does not exhibit any visible frost feature. On the contrary, anthropogenic features as fireplaces are able to record frost-related pedofeatures (Cremaschi et al., 2015). The LIA has instead triggered in the soil a variety of stable features related to intermittent freezing cycles. Such clear difference might suggest that other climate dynamics were in place during the cold phases preceding the LIA (for instance, the IACE). In this perspective, it might be plausible to characterise the LIA as a colder or drier period than the previous ones: lower temperatures in comparison with the other Holocene cold periods would have allowed more widespread episodes of seasonal frost. Holocene temperature anomalies reconstructed in the Southern Alps by Furlanetto et al. (2018) support this hypothesis suggesting a moderate shift towards lower temperatures in the LIA compared to other Holocene climatic phases. Moreover, a recent assessment of post-LGM permafrost distribution in the Mediterranean region suggests a widespread occurrence of soil frost in the LIA (Oliva et al., 2018). Similarly, a lessened amount of precipitation would have reduced ~~sensibly~~ the snow cover, well below the current thickness and down to only a few tens of centimetres (Zhang, 2005), weakening the thermal isolation of the soil below and allowing frost to take hold (Edwards et al., 2007b and references therein). A consequent shift downwards of the freezing front would plausibly have left more visible and stable features in the soils, while in less rigid and wetter phases they would only have suffered the consequences of more snow thawing upslope, especially a higher water discharge rate and in turn the activation of slope movements. The relationship between precipitations and slope processes is well studied in the Alps: today, where climate conditions are more severe lower rainfall thresholds are needed to trigger slope movements (Guzzetti et al., 2007). Considering the enhanced possibility of slope instability in cold environments, the absence of truncations in the upper soil unit confirms stable slope conditions and further supports a possible dry phase. While it is very difficult to assess past precipitation amount? rates, reconstructed temperatures from proxy data in the Alps seem to favour this idea (for comparison, see Badino et al., 2018; Furlanetto et al., 2018). Similar conditions have also been very recently postulated for the Northern Apennines (Regattieri et al., 2014; Mariani et al., 2019). The occurrence of other evidence confirming the climatic conditions in Mediterranean mountain ranges during the LIA confirms that soils and pedofeatures can reflect regional climatic conditions and they are not only triggered by local conditions and surface processes. The effect of forest clearance must be taken into account when discussing temperature in the topsoil. In fact, the presence of a forest cover greatly mitigates the effect of air temperature on the soil, with the canopy protecting the lower air strata and producing a warmer microclimate that reaches temperatures below zero with more difficulty (Körner. 2003). On the other hand, the canopy effect also prevents part of the snow accumulation, reducing its isolating power. In this area, the continuous presence since the Mesolithic of clearance events by fire and the more recent establishment of pasturelands (Castelletti et al., 2012b) probably prevented for long periods of time the reestablishment of a closed forest, leaving more open vegetations in which both these effects were probably greatly reduced.

VI. Conclusions

This study reconstructs climatic fluctuations throughout the Holocene on the basis of a soil polysequence the pedogenetic processes that occurred in a high mountain range throughout the Holocene. Moreover, we believe oOur study shows highlights it brings new evidence regarding on the importance of the LIA in the Alps as one of the main cold intervals after the LGM. While it is difficult to make assumptions based on indirect archives, it is plausible to infer, based on the evidence found in this study, that during the LIA the intensity of frost action might have been stronger compared to other Holocene cold episodes. An increase in ice formation could in turn be related to the occurrence of drier/colder conditions weakening snow deposition on the soil surface and favouring overall freezing conditions.

While soil archives are considered a low-mid resolution resource in palaeoclimatic studies (Yaalon, 1990), in this case the reconstruction of pedogenesis was the only reliable tool for recording cold intervals that occurred after the LGM in a non-glaciated area and their influence on surface processes. The study of soils and specifically micromorphology discloses important information on past climate, especially under the microscope, where evidence traces of processes triggered by specific climatic and environmental conditions (in this case atmospheric temperature) can be observed and put inside their proper placement in time (*sensu* Cremaschi et al., 2018). In environments where human actions started tuning surface processes earlier than expected in the Mid-Late Holocene, as suggested by recent studies (ArchaeoGLOBE Project, 2019), soil evidence also helps in disentangling natural and anthropogenic factors shaping the landscape in human-settled contexts. The absence of such specific deposits and landforms allowing the formation and conservation of soils and palaeosols would indeed render many of such reconstructions quite arduous, if not implausible. Finally, recent studies suggested that human actions started tuning surface processes earlier than expected in the Mid-Late Holocene (ArchaeoGLOBE Project, 2019); in this case, the study of soil also helps detangling natural and anthropogenic factors shaping the landscape in human-settled contexts.

References

Allison RJ (1996) Slope and slope processes. *Progress in Physical Geography* 20(4): 453-465.

Angelucci D, Cremaschi M, Negrino F and Pelfini M (1992) Il sito mesolitico di Dosso Gavia - Val di Gavia (Sondrio - Italia): evoluzione ambientale e popolamento umano durante l'Olocene antico nelle Alpi Centrali. *Preistoria Alpina* 28: 19–32.

ArchaeoGLOBE Project (2019) Archaeological assessment reveals Earth's early transformation through land use. *Science* 365: 897–902.

Arnaud F, Révillon S, Debret M, Revel M, Chapron E, Jacob J, Giguet-Covex C, Poulenard J and Magny M (2012) Lake Bourget regional erosion patterns reconstruction reveals Holocene NW European Alps soil evolution and palaeohydrology. *Quaternary Science Reviews* 51: 81-92.

Badino F, Ravazzi C, Vallè F, Pini R, Aceti A, Brunetti M, Champvillair E, Maggi V, Maspero F, Perego R and Orombelli G (2018) 8800 years of high-altitude vegetation and climate history at the Rutor Glacier forefield, Italian Alps. Evidence of middle Holocene timberline rise and glacier contraction. *Quaternary Science Reviews* 185: 41–68.

Baroni C and Orombelli G (1996) The Alpine "Iceman" and Holocene Climatic Change. *Quaternary Research* 46(1): 78 – 83.

Barry RG (1992) *Mountain weather and climate*. London: Routledge.

Bertolini G, Casagli N, Ermini L and Malaguti C (2004) Radiocarbon data on Lateglacial and Holocene landslides in the Northern Apennines. *Natural Hazards* 3: 645–662.

Bini A, Buoncristiani JF, Coutterand S, Ellwanger D, Felber M, Florineth D, Graf HR, Keller O, Schlüchter C and Schoeneich P (2009) *La Svizzera durante l'ultimo massimo glaciale (LGM), 1:500'000.* Ufficio federale di topografia swisstopo, Wabern.

Birkeland PW (1999) *Soils and Geomorphology*. New York: Oxford University Press.

Boardman J (1985) Comparison of Soils in Midwestern United States and Western Europe with the Interglacial Record. *Quaternary Research* 23(1): 62-75.

Boeckli L, Brenning A, Grube S and Noetzli J (2012) Permafrost distribution in the European Alps: calculation and evaluation of an index map and summary statistics. *The Cryosphere* 6: 807-820.

Bollati I, Cerrato R, Crosa Lenz B, Vezzola L, Giaccone E, Viani C, Zanoner T, Azzoni RS, Masseroli A, Pellegrini M, Scapozza C, Zerboni A and Guglielmin M (2018) Geomorphological map of the Val Viola Pass (Italy-Switzerland). *Geografia Fisica e Dinamica Quaternaria* DOI 10.4461/GFDQ.2018.41.2

Bradley RS (ed) (2015) *Palaeoclimatology (third edition)*. London: Academic Press.

Butler DR (1995) *Zoogeomorphology: Animals as Geomorphic Agents*. Cambridge, UK: Cambridge University Press.

Butler DR (2012) The impact of climate change on patterns of zoogeomorphological influence: examples from the Rocky Mountains of the Western U.S.A. *Geomorphology* 157-158: 183–191.

Butler DR (2018) Zoogeomorphology in the Anthropocene. *Geomorphology* 303: 146–154.

Calderoni G, Guglielmin M and Tellini C (1998) Radiocarbon dating and postglacial evolution, upper Valtellina and Livignese area (Sondrio, Central Italian Alps). *Permafrost and Periglacial Processes* 9: 275 – 284.

Carturan L, Baroni C, Carton A, Cazorzi F, Fontana GD, Delpero C, Salvatore MC, Seppi R and Zanoner T (2014) Reconstructing Fluctuations of La Mare Glacier (Eastern Italian Alps) in the Late Holocene. *Geografiska Annaler: Series A, Physical Geography* 96: 287–306.

Castelletti L, Caimi R and Tremari M (2012a) Ricerche archeologiche di superficie in Val Cavargna. In: Castelletti L and Motella de Carlo S (eds) *Il fuoco e la montagna. Archeologia del paesaggio dal Neolitico all'età moderna in Alta Val Cavargna*. Como: Università degli Studi dell'Insubria, pp. 79-88.

Castelletti L, Martinelli E, Motella de Carlo S and Procacci G (2012b) Archeologia del fuoco in Val Cavargna. In: Castelletti L and Motella de Carlo S (eds) *Il fuoco e la montagna. Archeologia del paesaggio dal Neolitico all'età moderna in Alta Val Cavargna*. Como: Università degli Studi dell'Insubria, pp. 137-185.

Castelletti L and Tremari M (2012) Edifici e tracce insediative in Val Cavargna. In: Castelletti L and Motella de Carlo S (eds) *Il fuoco e la montagna. Archeologia del paesaggio dal Neolitico all'età moderna in Alta Val Cavargna*. Como: Università degli Studi dell'Insubria, pp. 89-110.

Ceriani M and Carelli M (2000) *Carta delle precipitazioni massime, medie e minime del territorio alpino della Regione Lombardia*. Milano: Servizio Geologico, Ufficio Rischi Geologici Regione Lombardia.

Colucci RR, Boccali C, Zebre M and Guglielmin M (2016) Rock glaciers, protalus ramparts and pronival ramparts in the south-eastern Alps. *Geomorphology* 269: 112–121.

Compostella C, Trombino L and Caccianiga M (2012) Late Holocene soil evolution and treeline fluctuations in the Northern Apennines. *Quaternary International* 289: 46–59.

Compostella C, Mariani GS and Trombino L (2014) Holocene environmental history at the treeline in the Northern Apennines, Italy: A micromorphological approach. *The Holocene* 24(4): 393–404.

Cornell RM and Schwertmann U (2003) *The Iron Oxides*. Weinheim: Wiley.

Cremaschi M and Rodolfi G (1991) *Il suolo - Pedologia nelle scienze della Terra e nella valutazione del territorio*. Roma: La Nuova Italia Scientifica.

Cremaschi M, Mercuri AM, Torri P, Florenzano A, Pizzi C, Marchesini M and Zerboni A (2016) Climate change versus land management in the Po Plain (Northern Italy) during the Bronze Age: New insights from the VP/VG sequence of the Terramara Santa Rosa di Poviglio. *Quaternary Science Reviews* 136: 153–172.

Cremaschi M and Nicosia C (2012) Sub-Boreal aggradation along the Apennine margin of the Central Po Plain: geomorphological and geoarchaeological aspects. *Geomorphologie* 2: 155–174.

Cremaschi M, Trombino L and Zerboni A (2018) Palaeosoils and relict soils, a systematic review. In: Stoops G, Marcelino V and Mees F (eds) *Interpretation of Micromorphological Features of Soils and Regoliths. Second edition*. Amsterdam: Elsevier, pp. 863–894.

Cremaschi M, Zerboni A, Nicosia C, Negrino F, Rodnight H and Spötl C (2015) Age, soil-forming processes, and archaeology of the loess deposits at the Apennine margin of the Po Plain (northern Italy). New insights from the Ghiardo area. *Quaternary International* 376: 173-188

Cremonese E, Gruber S, Phillips M, Pogliotti P, Boeckli L, Noetzli J, Suter C, Bodin X, Crepaz A, Kellerer-Pirklbauer A, Lang K, Letey S, Mair V, Morra di Cella U, Ravanel L, Scapozza C, Seppi R and Zischg A (2011) Brief Communication: "An inventory of permafrost evidence for the European Alps". *The Cryosphere* 5: 651-657.

Crosta GB, Frattini P and Agliardi F (2013) Deep seated gravitational slope deformations in the European Alps. *Tectonophysics* 605: 13–33.

Crouvi O, Amit R, Enzel Y, Porat N and Sandler A (2008) Sand dunes as a major proximal dust source for late Pleistocene loess in the Negev Desert, Israel. *Quaternary Research* 70: 275–282.

Deline P and Orombelli G (2005) Glacier fluctuations in the western Alps during the Neoglacial, as indicated by the Miage morainic amphitheatre (Mont Blanc massif, Italy). *Boreas* 34: 456-467.

Duchaufour P (1977) *Précis de pédologie*. Paris: Masson.

Duchaufour P (1983) *Pédologie. 1. Pédogenèse et classification*. Paris: Masson.

Dumanski JA and St-Arnaud RJ (1966) A micropedological study of eluviated horizons. *Canadian Journal of Soil Science* 46: 287–292.

Edwards TL, Crucifix M and Harrison SP (2007a) Using the past to constrain the future: how the palaeorecord can improve estimates of global warming. *Progress in Physical Geography* 31(5): 481–500.

Edwards AC, Scalenghe R and Freppaz M (2007b) Changes in the seasonal snow cover of alpine regions and its effect on soil processes: A review. *Quaternary International* 162–163: 172–181.

Federici PR (2005) Aspetti e problemi della glaciazione pleistocenica nelle Alpi Apuane. *Istituto Italiano di Speleologia Mem.* 18(2): 19–32.

Federici PR, Ribolini A and Spagnolo M (2017) Glacial history of the Maritime Alps from the last Glacial maximum to Little Ice Age. In: Hughes PD and Woodward JC (eds) *Quaternary glaciation in Mediterranean Mountains*. London: Geological Society, Special Publications 433, pp. 137–159.

Fedoroff N (1997) Clay illuviation in Red Mediterranean soils. *Catena* 28: 171–189.

Fischer P, Hilgers A, Protze J, Kels H, Lehmkuhl F and Gerlach R (2012) Formation and geochronology of Last Interglacial to Lower Weichselian loess/palaeosol sequences – case studies from the Lower Rhine Embayment, Germany. *Quaternary Science Journal* 61(1): 48–63.

Food and Agriculture Organization (FAO) (2006) *Guidelines for Soil Description. 4th Edition*. Rome: FAO.

Food and Agriculture Organization (FAO) (2014) *World reference base for soil resource 2014. World Soil Resources Reports. N° 106*. FAO, Rome: FAO.

Furlanetto G, Ravazzi C, Pini R, Vallè F, Brunetti M, Comolli R, Novellino MD, Garozzo L and Maggi V (2018) Holocene vegetation history and quantitative climate reconstructions in a high-elevation oceanic district of the Italian Alps. Evidence for a middle to late Holocene precipitation increase. *Quaternary Science Reviews* 200: 212–236.

Gazzolo T and Pinna M (1973) *La nevosità in Italia nel quarantennio 1921-1960*. Rome: Istituto Poligrafico dello Stato.

Giraudi C, Bodrato G, Ricci Lucchi M, Cipriani M, Villa IM, Giaccio B and Zuppi GM (2011) Middle and Late Pleistocene Glaciations in the Campo Felice basin (Central Apennines - Italy). *Quaternary Research* 75: 219 – 230.

Grandi G (2012) Popolazione, attività minerarie e siderurgiche, uso dei boschi e carbonaie tra il XV e il XIX secolo in Val Cavargna. In: Castelletti L and Motella de Carlo S (eds) *Il fuoco e la montagna. Archeologia del paesaggio dal Neolitico all'età moderna in Alta Val Cavargna*. Como: Università degli Studi dell'Insubria, pp. 21-36.

Grosjean M, Suter PJ, Trachsel M and Wanner H (2007) Ice-borne prehistoric finds in the Swiss Alps reflect Holocene glacier fluctuations. *Journal of Quaternary Science* 22(3): 203–207.

Guzzetti F, Peruccacci S, Rossi M and Stark CP (2007) Rainfall thresholds for the initiation of landslidesin central and southern Europe. *Meteorology and Atmospheric Physics* 98: 239–267.

Henry HAL (2007) Soil freeze–thaw cycle experiments: Trends, methodological weaknesses and suggested improvements. *Soil Biology and Biochemistry* 39: 977–986.

Hughes PD, Woodward JC, van Calsteren PC and Thomas LE (2011) The glacial history of the Dinaric Alps, Montenegro. *Quaternary Science Reviews* 30(23–24): 3393–3412.

Jenny H (1941) *Factors of Soil Formation*. New York: McGraw-Hill.

Knight J and Harrison S (2009) Periglacial and paraglacial environments: a view from the past into the future. In: Knight J and Harrison S (eds) *Periglacial and Paraglacial Processes and Environments*. London: Geological Society, Special Publications, 320, pp. 1-4.

~~Kooistra MJ and Pulleman MM (2018) Features Related to Faunal Activity. In: Stoops G, Marcelino V and Mees F (eds) *Interpretation of Micromorphological Features of Soils and Regoliths. Second edition*. Amsterdam: Elsevier, pp. 447–470.~~

Körner C (2003) *Alpine Plant Life. Second Edition*. Berlin: Springer.

Kuhlemann J, Gachev E, Gikov A, Nedkov S, Krumrei I and Kubik P (2013) Glaciation in the Rila mountains (Bulgaria) during the Last Glacial Maximum, *Quaternary International* 293: 51–62.

Kullman L and Öberg L (2009) Post - Little Ice Age tree line rise and climate warming in the Swedish Scandes: a landscape ecological perspective. *Journal of Ecology* 97: 415–429.

Kutzbach JE (1976) The nature of climate and climatic variations. *Quaternary Research* 6: 471–480.

Loso MG, Doak DF and Anderson RS (2014) Lichenometric dating of Little Ice Age glacier moraines. *Geografiska Annaler: Series A, Physical Geography* 96: 21–41.

Magny M, Vannière B, Zanchetta G, Fouache E, Touchais G, Petrika L, Coussot C, Walter-Simonnet AV and Arnaud F (2009a) Possible complexity of the climatic event around 4300–3800 cal. BP in the central and western Mediterranean. *The Holocene* 19: 823–833.

Magny M, Peyron O, Gauthier E, Roueche Y, Bordon A, Billaud Y, Chapron E, Marguet A, Pétrequin P and Vannière B (2009b) Quantitative reconstruction of climatic variations during the Bronze and early Iron ages based on pollen and lake-level data in the NW Alps, France. *Quaternary International* 200(1-2): 102–110.

Mariani GS, Cremaschi M, Zerboni A, Zuccoli L and Trombino L (2018) Geomorphology of the Mt. Cusna Ridge (Northern Apennines, Italy): evolution of a Holocene landscape. *Journal of Maps* 14(2): 392-401. DOI: 10.1080/17445647.2018.1480976

Mariani GS, Compostella C and Trombino L (2019) Complex climate-induced changes in soil development as markers for the Little Ice Age in the Northern Apennines (Italy). *Catena* 181. DOI: 10.1016/j.catena.2019.104074

Mauri A, Davis BAS, Collins PM and Kaplan JO (2015) The climate of Europe during the Holocene: a gridded pollen-based reconstruction and its multi-proxy evaluation. *Quaternary Science Reviews* 112: 109–127.

Mayewski PA, Rohling EE, Stager JC, Karlén W, Maasch KA, Meeker LD, Meyerson EA, Gasse F, van Kreveld S, Holmgren K and Lee-Thorp J (2004) Holocene climate variability. *Quaternary Research* 62(3): 243–255.

McKeague JA, Brydon JE and Miles NM (1971) Differentiation of forms of extractable iron and aluminium in soils. *Soil Science Society of America Proceedings* 35: 33–38.

Mehra OP and Jackson ML (1960) Iron oxide removal from soils and clays by a dithionite-citrate system buffered with sodium bicarbonate. *Clays and Clay Minerals* 7: 317–327.

Munsell Color® (1994) *Munsell soil color charts.* New Windsor, NY: Munsell Color.

Murphy CP (1986) *Thin Section Preparation of Soils and Sediments*. Herts, UK: AB Academic Publishers.

Nicholson SE (1988) Land surface atmosphere interaction: physical processes and surface changes and their impact. *Progress in Physical Geography* 12(1): 36-65.

Nicolussi K (2013) Die historischen Vorstöße und Hochstände des Vernagtferners 1600-1850 AD. *Zeitschrift für Gletscherkunde und Glazialgeologie* 45-46: 9–23.

Nicolussi K, Kauffman M, Patzelt G, van der Plicht J and Thurner A (2005) Holocene tree-line variability in the Kauner valley, central Eastern Alps, indicated by dendrochronological analysis of living trees and subfossil logs. *Vegetation History and Archaeobotany* 14: 221–234.

Oliva M, Zebre M, Guglielmin M, Hughes PD, Ciner A, Vieira G, Bodin X, Andrés N, Colucci RR, Garcia-Hernandez C, Mora C, Nofre J, Palacios D, Perez-Alberti A, Ribolini A, Ruiz-Fernandez J, Sarikaya MA, Serrano E, Urdea P, Valcarcel M, Woodward JC and Yildirim C (2018) Permafrost conditions in the Mediterranean region since the Last Glaciation. *Earth Science Reviews* 185: 397 ‐ 436.

Pelfini M, Leonelli G, Trombino L, Zerboni A, Bollati I, Merlini A, Smiraglia C and Diolaiuti C (2014) New data on glacier fluctuations during the climatic transition at ~4,000 cal. year BP from a buried log in the Forni Glacier forefield (Italian Alps). *Rend. Fis. Acc. Lincei* 25: 427–437.

Plunkett G and Swindles GT (2008) Determining the Sun's influence on Lateglacial and Holocene climates: a focus on climate response to centennial-scale solar forcing at 2800 cal. BP. *Quaternary Science Reviews* 27(1–2): 175–184.

Porter SC and Orombelli G (1985) Glacier contraction during the middle Holocene in the western Italian Alps: Evidence and implications. *Geology* 13(4): 296–298.

Regattieri E, Zanchetta G, Drysdale RN, Isola I, Hellstrom JC and Dallai L (2014) Lateglacial to Holocene trace element record (Ba, Mg, Sr) from Corchia Cave (Apuan Alps, central Italy): paleoenvironmental implications. *Journal of Quaternary Science* 29(4): 381-392.

Reimer PJ, Bard E, Bayliss A, Beck JW, Blackwell PG, Bronk Ramsey C, Buck CE, Cheng H, Edwards RL, Friedrich M, Grootes PM, Guilderson TP, Haflidason H, Hajdas I, Hatté C, Heaton TJ, Hoffmann DL, Hogg AG, Hughen KA, Kaiser KF, Kromer B, Manning SW, Niu M, Reimer RW, Richards DA, Scott EM, Southon JR, Staff RA, Turney CSM and van der Plicht J (2013) IntCal13 and Marine13 radiocarbon age calibration curves 0–50,000 years cal BP. *Radiocarbon* 55(4): 1869–1887.

Schwertmann U (1973) Use of oxalate for Fe extraction from soils. *Canadian Journal of Soil Science* 53: 244–246.

Sevink J and de Waal RW (2010) Soil and humus development in drift sands. In: Fanta J and Siepel H (eds) *Inland Drift Sand Landscapes*. Zeist, Netherlands: KNVV Publishing, pp. 107–134.

Soil Survey Staff (2014) *Keys to Soil Taxonomy. 12th ed.* Washington, DC: USDA-Natural Resources Conservation Service.

Spalla MI, Di Paola S, Gosso G, Siletto GB and Bistacchi A (2002) Mapping tectono-metamorphic histories in the Lake Como basement (Southern Alps, Italy). *Memorie di Scienze Geologiche* 54: 149-167.

Stoops G (2003) *Guidelines for analysis and description of soil and regolith thin sections*. Madison, Wisconsin: Soil Science Society of America.

Stoops G, Marcelino V and Mees F (eds) (2018) *Interpretation of Micromorphological Features of Soils and Regoliths. Second edition*. Amsterdam: Elsevier.

Van Ranst E, Wilson MA and Righi D (2018) Spodic materials. In: Stoops G, Marcelino V and Mees F (eds) *Interpretation of Micromorphological Features of Soils and Regoliths. Second edition*. Amsterdam: Elsevier, pp. 633–662.

Van Vliet-Lanoë B (1987) Dynamique périglaciaire actuelle et passée. Apport de l'étude micromorphologique et de l'expérimentation. *Bulletin A.F.E.Q.* 2: 113–132.

Van Vliet-Lanoë B (1998) Frost and soils: implications for palaeosols, palaeoclimates and stratigraphy. *Catena* 34: 157–183.

Van Vliet-Lanoë B, Coutard JP and Pissart A (1984) Structures caused by repeated freezing and thawing in various loamy sediments. A comparison of active, fossil and experimental data. *Earth Surface Processes and Landforms* 9: 553–565.

Van Vliet-Lanoë B and Fox CA (2018) Frost action. In: Stoops G, Marcelino V and Mees F (eds) *Interpretation of Micromorphological Features of Soils and Regoliths. Second edition*. Amsterdam: Elsevier, pp. 575–603.

Vepraskas MJ, Lindbo DL and Stolt MH (2018) Redoximorphic Features. In: Stoops G, Marcelino V and Mees F (eds) *Interpretation of Micromorphological Features of Soils and Regoliths. Second edition*. Amsterdam: Elsevier, pp. 425–446.

Wanner H, Solomina O, Grosjean M, Ritz SP and Jetel M (2011) Structure and origin of Holocene cold events. *Quaternary Science Reviews* 30: 3109–3123.

Waroszewski J, Egli M, Brandová D, Christl M, Kabala C, Malkiewicz M, Kierczak J, Glina B and Jezierski P (2018) Identifying slope processes over time and their imprint in soils of medium - high mountains of Central Europe (the Karkonosze Mountains, Poland). *Earth Surface Processes and Landforms* 43: 1195–1212.

Yaalon DH (1990) The relevance of soils and paleosols in interpreting past and ongoing climatic changes. *Palaeogeography Palaeoclimatology Palaeoecology* 82: 63 – 64.

Zanchetta G, Regattieri E, Isola I, Drysdale RN, Bini M, Baneschi I and Hellstrom JC (2016) The so-called "4.2 event" in the Central Mediterranean and its climatic teleconnections. *Alpine Mediterranean Quaternary* 29(1): 5 – 17.

Zerboni A, Trombino L and Cremaschi M (2011) Micromorphological approach to polycyclic pedogenesis on the Messak Settafet plateau (central Sahara): Formative processes and palaeoenvironmental significance. *Geomorphology* 125: 319-335.

Zerboni A, Trombino L, Frigerio C, Livio F, Berlusconi A, Michetti AM, Rodnight H and Spötl C (2015) The loess-palaeosol sequence at Monte Netto: a record of climate change in the Upper Pleistocene of the central Po Plain, northern Italy. *Journal of Soils and Sediments* 15: 1329–1350.

Zerboni A and Nicoll K (2018) Enhanced zoogeomorphological processes in North Africa in the human-impacted landscapes of the Anthropocene. Geomorphology 331: 22-35.

Zhang T (2005) Influence of the seasonal snow cover on the ground thermal regime: an overview. *Reviews of Geophysics* 43: RG4002.

Captions

Figure 1. (A) Hillshade of the central sector of Southern Alps indicating the location of the study area (the inset indicates its position in northern Italy). (B) Satellite view of the study area (source: Google Earth™); the star indicates the position of the soil profile.

Figure 2. (A) General view of the study area during the opening of the test trench. In the foreground the high portion of the DSGSD is visible to the right; the DSGSD is broken downslope to the left by a morphological trench associated with a counterscarp. In the background the peak of Mt. Pizzo di Gino and its southern slope are visible to the left. (B) Picture of the investigated polycyclic soil sequence indicating the position of soil horizons and samples for analyses (squares: blocks for thin sections; triangles: samples for chemical-physical analyses; dots: samples for radiocarbon dating).

Figure 3. Results of chemical-physical analyses: on the left, curves of grain size distribution (after H_2O_2 and HCl treatments); on the right, chemical determinations of Fe content. Key: Fe(o): amorphous iron; Fe(d): free iron; Fe(t): total iron.

Figure 4. Micromorphological features of the investigated soil horizons: a) well developed yellowish fabric devoid of iso-oriented features in the intermediate unit (2Bs horizon; 2x, PPL); b) depleted soil mass in the lower unit (3Et horizon; 2x, PPL); c) microlaminated clay coatings in the eluvial horizon of the lower unit (3Et horizon; 10x, PPL); d) same as c), in XPL.

Figure 5. Frost related features of the investigated soil horizons: a) horizontal planar voids in the upper unit (A2 horizon; 4x, PPL); b) groups of circular vesicles ~~around horizontal planar voids~~ in the upper unit (A2 horizon; 10x, PPL); c) horizontal iso-oriented mica fragments in the fabric of the upper unit (Bw horizon, 10x; XPL); d) passage features produced by ~~earthworms~~ beetle larvae ~~(possibly *Enchytraeidae*: Kooistra and Pulleman, 2018)~~ around undisturbed planar voids (A2 horizon; 4x, PPL).

Table 1. Field and chemical properties of the described soil sequence.

Table 2. Micromorphological descriptions of soil thin sections. G: gravel size; VCS: very coarse sand size; CS: coarse sand size; MS: medium sand size; FS: fine sand size; VFS: very fine sand size; S: silt size. Abundance: very dominant – >70%; dominant – 50–70%; frequent – 30–50%; common – 15–30%; few – 5–15%; very few – <5%; weak.: weakly; mod.: moderately; str.: strongly.

Table 3. Summary of microscopic properties of investigated soil horizons (full micromorphological data are in Supplementary Materials). Frost related pedofeatures in *italics*.